Table 1 Clinical summary of eight *PAX8* mutation carriers.

Variable	Family 1 L16P			Family 2 F20S		Family 3 D46fs		Family 4 R133Q	Reference
	Patient 1	Patient 2	Patient 3	Patient 4	Patient 5	Patient 6	Patient 7	Patient 8	
Age (years), sex	11, F	8, M	41, F	5, F	38, F	10, M	39, M	10, F	
Newborn screening	Negative	Negative	Not tested	Positive	Not tested	Positive	Not tested	Positive	
Age at diagnosis (years)	0.5	4	12	0.1	34	0.1	39	0.1	
Thyroid function									
Age at evaluation (years)	3	4	12	0.1	34	6	39	5	
Serum TSH (mU/l)	**19.7**	**16.3**	**710**	**183**	**161**	**13.8**	**5.6**	**18.0**	0.5–5.0
Serum-free T_4 (ng/dl)	NA[a]	1.0	NA	1.1	**0.3**	0.9	**0.8**	NA	0.9–1.8
Serum Tg (ng/ml)	13	24	NA	NA	**360**	28	**32**	NA	<30
Thyroid ultrasonography									
Age at evaluation	9	4	NA	3	34	6	39	13	
Size (SDS)	**−3.1**	−1.7	NA	**−3.5**	**−3.3**	−1.3	**−3.0**	**−3.5**	−2 to +2
Echogenicity	Normal	Normal	NA	Normal	Normal	**Low**	**Low**	**Low**	Normal
Thyroid growth	**Absent**	NA	NA	**Absent**	NA	Present	NA	NA	Present
^{123}I uptake at 24 h (%)	12.3	10.8	NA	NA	NA	22.6	NA	20.6	8–40
$KClO_4$ discharge rate (%)	8.3	0.0	NA	NA	NA	**12.8**	NA	NA	<10

NA, not available; T_4, thyroxine; Tg, thyroglobulin. Abnormal values/findings are given in boldface.
[a]Total thyroxine was 7.6 μg/dl.

electrophoresis and transferred to a nylon membrane. The biotin-labeled probe was detected with the Light-shift chemiluminescent EMSA kit (Pierce).

Transactivation assays

Cells grown in 96-well plates with about 80% confluence were cotransfected with 50 ng of the luciferase reporter driven by the *TG* promoter (*TG*-luc (12)), and various doses of the effector plasmids or the empty vector. The amount of transfected plasmid was kept constant by adding the empty vector. Twenty-four hours after transfection, we measured firefly luciferase activities using ONE-Glo Luciferase Assay System (Promega). Luciferase activities were represented relative to the activity obtained by transfection of empty vector and were expressed as mean ± S.E.M. Welch's *t*-test was used for statistical comparisons with significance at $P<0.05$.

Results

Clinical histories

Clinical phenotypes of eight mutation carriers (Patients 1–8) belonging to four families (Families 1–4) are summarized in Table 1. The pedigrees are shown in Fig. 1.

Family 1 The proband (Patient 1; a girl) had a normal blood spot TSH level (9 mU/l; cutoff level, 10) at newborn screening for CH. Her first thyroid function test was conducted at age 6 months because her mother (Patient 3) had childhood hypothyroidism. At this point, she had a high serum TSH level (14 mU/l; reference, 0.5–5.0) with a normal free thyroxine (T_4) level (1.1 ng/dl; reference, 0.9–1.8). She had no CH-related symptom and was growing and developing normally. At age 9 months, levothyroxine (L-T_4) replacement was started because her serum TSH level increased to 22.3 mU/l. At age 3 years, we reassessed her thyroid status with transient discontinuation of therapy and confirmed permanent CH (TSH, 19.7 mU/l; T_4, 7.6 μg/dl (reference, 9.3–17.1); Tg, 13 ng/ml). Ultrasonography showed a normoechoic hypoplastic thyroid (−2.5 S.D. (16); Supplementary Figure 1, see section on supplementary data given at the end of this article). ^{123}I uptake at 24 h was 12.3% (reference, 8–40), and perchlorate discharge rate was 8.3% (reference, 0–10). Repeated ultrasonography at age 9 years showed thyroid hypoplasia (−3.1 S.D.; Supplementary Figure 1).

Patient 2, a younger brother of the proband, also had a negative result in newborn screening. At age 2 months, his first thyroid function test showed a slightly high serum TSH level (7.3 mU/l) with a normal T_4 level (11.2 μg/dl). At age 4 years, his second thyroid function test revealed subclinical hypothyroidism (TSH, 16.3 mU/l; free T_4, 1.0 ng/dl; Tg, 24 ng/ml).

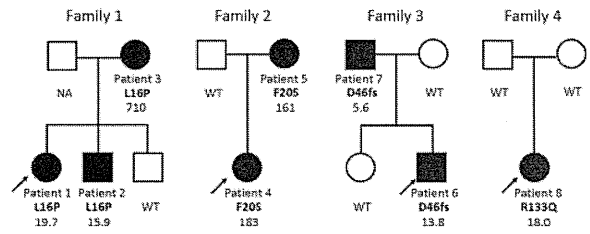

Figure 1 Pedigrees of four families with *PAX8* mutations are shown. Values presented below each symbol indicate TSH levels as expressed in milliunits per liter (reference, 0.5–5.0). Family studies showed that all mutation carriers had high serum TSH levels. Squares, men; circles, women; solid symbols, affected by hypothyroidism; open symbols, unaffected.

Ultrasonography showed a slightly hypoplastic thyroid (−1.7 S.D.; Supplementary Figure 1). ^{123}I uptake was normal (10.8% at 24 h), and no discharge after perchlorate challenge was observed. At this point, L-T_4 replacement was started.

Patient 3, a mother of the proband, was born before the implementation of newborn screening for CH. She was first evaluated for her thyroid function at age 12 years due to mild mental retardation and short stature. She had a markedly high serum TSH level (710 mU/l) with no thyroid autoantibodies. Thyroid scintigraphy showed a normally located thyroid gland with reduced radioiodine uptake (detailed data were unavailable). She has been receiving L-T_4 replacement therapy after the diagnosis.

Family 2 The proband (Patient 4; a girl) was born by cesarean section due to fetal distress. Newborn screening for CH revealed a high blood spot TSH level (79.6 mU/l). At age 9 days, she had a high serum TSH level (183 mU/l) with a normal serum-free T_4 level (1.1 ng/dl). Although her primary physician noted no CH-related symptoms, her distal femoral epiphyseal ossification center was absent, suggesting her hypothyroid status. Ultrasonography showed hypoplastic thyroid (−2.5 S.D.; Supplementary Figure 1). Immediately after the evaluation, L-T_4 replacement was started. At age 3 years, repeated ultrasonography showed hypoplastic thyroid (−3.5 S.D.) with normal echogenicity (Supplementary Figure 1).

Patient 5, a mother of the proband, was born before the implementation of newborn screening for CH. She had normal height (153 cm), had no obvious intellectual problem, and had no apparent symptoms of hypothyroidism. We evaluated her thyroid function at age 34 years as a family study of the mutation. She had an elevated serum TSH level (161 mU/l), a low free T_4 level (0.3 ng/dl), and a high Tg level (360 ng/ml). A hypoplastic normoechoic thyroid (volume, 1.4 ml) was shown by ultrasonography (Supplementary Figure 1). Thereafter, she has been receiving L-T_4 replacement therapy.

Family 3 The proband (Patient 6; a boy) had a high blood spot TSH level (17.5 mU/l) at newborn screening. At age 41 days, thyroid function test showed a slightly high serum TSH level (15.6 mU/l) with a marginally low free T_4 level (0.9 ng/dl). He did not have CH-related symptoms. Ultrasonography revealed a hypoplastic hypoechoic thyroid (−2.5 S.D.; Supplementary Figure 1). L-T_4 replacement was started. At age 6 years, we reevaluated his thyroid status with transient discontinuation of treatment. He had permanent CH with serum TSH 13.8 mU/l, free T_4 0.9 ng/dl, and Tg 28 ng/ml. He had normal ^{123}I uptake (19.7% at 24 h), although perchlorate discharge rate was slightly high (12.8%). Ultrasonography showed a normal-sized hypoechoic gland (−1.3 S.D.; Supplementary Figure 1).

Patient 7, a father of the proband, was born before the implementation of newborn screening. He had normal height (171 cm), had no intellectual problems, and was euthyroid physically. We evaluated his thyroid status at age 39 years as a family study of the mutation. He had a slightly high serum TSH level (5.6 mU/l), a slightly

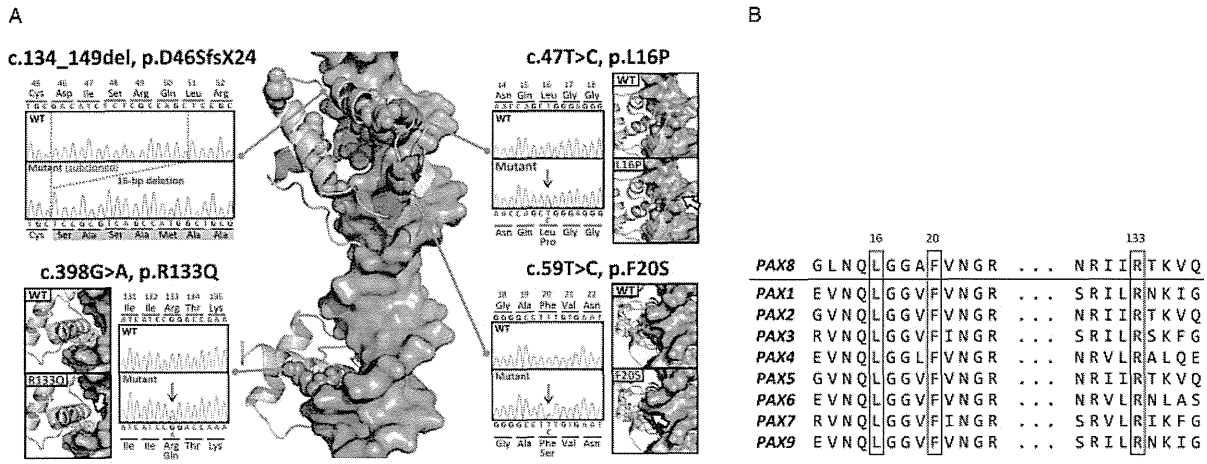

Figure 2 Location and impact of four novel *PAX8* mutations. (A) Three-dimensional structure of the DNA-binding paired domain (colored in gold) and its target DNA (colored in silver) based on the crystal structure data of PAX6–DNA complex. The domain consists of two β-sheets and six α-helices. Side chains of residues corresponding to 11 missense mutations (previously reported ones in turquoise (n=8) and novel ones found in this study in orange (n=3)) are shown as spheres. The eight previous mutations are located among three α-helices (α1–α3), whereas the three novel ones (L16P, F20S, and R133Q) are located outside the region. The D46fs mutation deletes normal protein sequence after the α1 helix. Representative chromatograms of each novel mutation are shown, along with the results of computational modeling of mutant structures. Note that the three missense mutations are predicted to affect protein–DNA interaction (indicated by white arrows). (B) Single-letter amino acid ClustalW alignments of residues surrounding Leu16, Phe20, and Arg133. The mutated residues, which are conserved in the Pax gene family, are colored in red.

low free T_4 level (0.8 ng/dl), and a slightly high Tg level (32 ng/ml). Ultrasonography showed a hypoplastic thyroid (volume, 5.4 ml) with low echogenicity (Supplementary Figure 1).

Family 4 The proband (Patient 8; a girl) had a high blood spot TSH level (40.6 mU/l) at newborn screening. She had no CH-related symptoms. The size of distal femoral epiphyseal ossification center was normal. Thyroid function test showed a high serum TSH level (33.2 mU/l) accompanied by a normal free T_4 level (1.4 ng/dl). She had been followed without treatment because her free T_4 levels were normal but was finally started on L-T_4 replacement at age 10 months (TSH, 13.9 mU/l; free T_4, 1.1 ng/dl). Reassessment of her thyroid status with discontinuing therapy at age 5 years confirmed permanent CH (TSH, 18.0 mU/l; free T_4, 1.2 ng/dl). ^{123}I uptake was normal (20.6% at 24 h). Perchlorate discharge test was not performed. Thyroid ultrasonography performed at age 13 years showed a hypoplastic gland (−3.5 S.D.) with low echogenicity (Supplementary Figure 1).

Mutation detection

We identified four novel heterozygous *PAX8* mutations in the four probands, including three missense mutations (c.47T>C, p.L16P in Family 1; c.59T>C, p.F20S in Family 2; c.398G>A, p.R133Q in Family 4) and one frameshift mutation (c.134_149del, p.D46SfsX24 in Family 3) (Fig. 2A). The four mutations were located in the paired domain (Fig. 2A) and were absent in 100 control individuals. Leu16, Phe20, and Arg133 are conserved among the PAX family genes (Fig. 2B). Computational modeling of the missense mutants predicted that they cause loss of contacts between the paired domain and its target DNA (Fig. 2A). Family studies revealed that the mutation was transmitted by either father or mother in three families (Families 1–3) and occurred *de novo* in Family 4 (Fig. 1).

In vitro *functional analyses*

To clarify the molecular pathogenesis of each mutant *PAX8*, we conducted a series of *in vitro* functional analyses using the human cervical cancer-derived HeLa cell line. Western blotting of myc-tagged PAX8 proteins showed that the protein expression level of D46fs was negligible, whereas those of the remaining three (L16P, F20S, and R133Q) were comparable with that of WT (Fig. 3A, left panel). When we treated transfected cells with the proteasome inhibitor MG132, we could detect the myc-tagged D46fs mutant, of which molecular weight was about 10 kDa, suggesting that the mutant protein was degraded via the proteasome-dependent pathway (Fig. 3A, right panel). Visualization of subcellular localization of the EGFP-tagged PAX8 proteins revealed that L16P, F20S, and R133Q were localized in the nucleus and were colocalized normally with TTF1, another thyroid-specific transcription factor (Fig. 3B). Electrophoretic mobility shift assay (EMSA) with two PAX8 response elements (oligo-CT and oligo-C) showed abrogated DNA-binding abilities of L16P, F20S, and R133Q on the two elements (Fig. 3C).

We assessed the effect of each mutation on target gene transactivation using a luciferase reporter driven by the *TG* promoter. To recapitulate interaction between WT and mutant PAX8, and interaction between PAX8 and TTF1 (i.e. synergistic transactivation (17)), various patterns of cotransfection were tested: mutant PAX8 only or WT-mutant cotransfection, each with or without coexpressed TTF1. In the absence of TTF1, the four mutants alone showed negligible transactivation (Fig. 3D, gray bars). Transactivating capacities measured by WT-mutant cotransfection (WT 5 ng; mutant 5 ng) were significantly lower than that derived from 10 ng of WT and were comparable with that derived from 5 ng of WT (Fig. 3D, stripe bars). This indicates that each mutant did not interfere with the transactivation of WT in WT-mutant cotransfection. In the presence of coexpressed TTF1, L16P, F20S, and R133Q had partial transactivating capacities, while D46fs did not (Fig. 3E, gray bars). However, when the four mutants were further cotransfected with WT PAX8 (WT 5 ng; mutant 5 ng), the transactivation levels of *TG*-luc were significantly lower than that derived from 10 ng of WT and were again comparable with that derived from 5 ng of WT (Fig. 3E, stripe bars).

Discussion

The thyroid phenotypes of the eight mutation carriers were considerably variable, regarding i) thyroid function (overt to subclinical hypothyroidism), ii) gland size (small to normal), and iii) gland echogenicity (low to normal). It is noteworthy that chronological changes were observed in several cases. Patients 1 and 2 had normal blood spot TSH levels in newborn screening but developed hypothyroidism thereafter. One similar screening-negative case has been described in the literature (10). As for Patient 1, thyroid ultrasonography was performed sequentially at ages 3 and 9 years and showed that her thyroid grew only minimally. This finding is consistent with our previous clinical observation suggesting that thyroid follicular growth is sensitive to a *PAX8* mutation (18). Another observation implying the chronological phenotypic changes in mutation carriers is the paradoxical clinical history of Patient 5. She presumably had compensated hypothyroidism in her childhood because she had apparently normal adult height and intelligence. Thus, her overt hypothyroidism, which was confirmed at age 34 years, should have developed in adulthood. Collectively, we presume that deleterious effects of *PAX8*

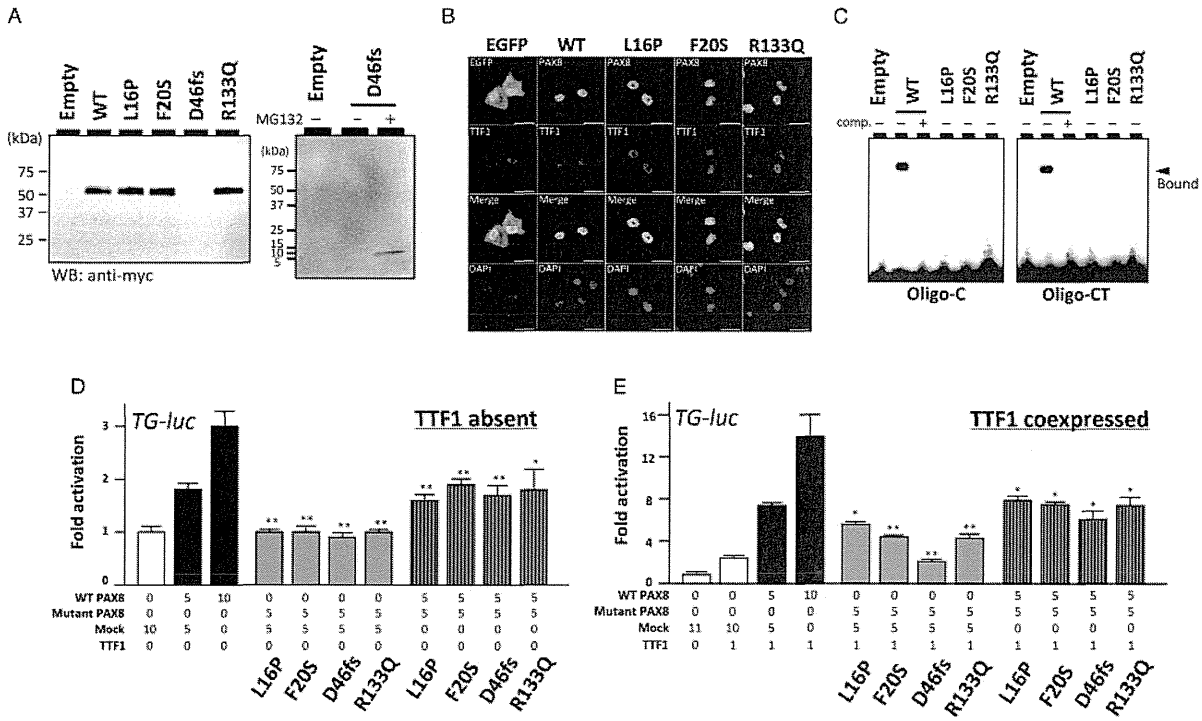

Figure 3 Functional characterization of four novel *PAX8* mutations. (A) Protein expression levels of myc-tagged PAX8 (wild type (WT) or mutant) were assessed by western blotting using a monoclonal anti-myc antibody. The protein expression level of D46fs was negligible, while those of the remaining three were comparable with that of WT (left panel). The D46fs mutation could be detected by western blotting with use of cell lysate extracted from MG132-treated HeLa cells (right panel), indicating that the mutation was degraded via proteasome-dependent pathway. (B) Subcellular localization analyses. Each enhanced green fluorescent protein-tagged PAX8 construct (WT or mutant) was cotransfected with red fluorescent protein-tagged thyroid transcription factor-1 (TTF1). Merged images show colocalization of TTF1 and each PAX8 protein. Bars indicate 50 μm. (C) DNA binding abilities of each PAX8 protein on two PAX8 response elements (oligo-CT and oligo-C) were tested by electrophoretic mobility shift assays. WT showed specific binding to the elements, which was competed by excess amount of cold competitors. Each mutant showed no binding on these two elements. (D and E) Transactivation activities of each PAX8 protein were assessed with use of the *TG*-luc reporter. HeLa cells grown in a 96-well plate were transfected with indicated amount (in nanogram) of the effector plasmid(s). Firefly luciferase activities were represented relative to the activity of the empty vector. Panel D displays the results comparing WT (black) and the four mutants (gray) in the absence of TTF1. WT transactivated the *TG*-luc in a dose-dependent manner. The four mutants showed negligible transactivating capacities. WT-mutant contransfection experiments showed no dominant negative effect. Panel E shows the results obtained in the presence of coexpressed TTF1 (1 ng). In this condition, three missense mutants showed various levels of transactivation, whereas D46fs remained nonfunctional. However, the transactivation levels derived from WT-mutant cotransfection (5 ng each) were comparable to that of WT only (5 ng). Data are representative of three independent experiments (each performed in quadricate) with similar results. Values are mean±S.E.M. The results of mutant-only transfection (5 ng) were compared with that of equimolar WT (5 ng), while those of WT-mutant cotransfection (total amount 10 ng) were compared with that of equimolar WT (10 ng). $^{*}P<0.05$, $^{**}P<0.01$.

mutations can exacerbate over time, resulting in significant chronological changes in disease phenotypes.

In this study, two types of *PAX8* mutations were found: mutations with defective DNA binding (L16P, F20S, and R133Q) and a mutation with defective protein stability (D46fs). The former type seems to be the predominant mechanism of *PAX8* mutations: ten out of 12 previously reported mutations are amino acid-altering ones located in the paired domain (4, 7, 8, 9, 10, 11, 12, 13). The paired domain consists of two β-turns (β1 and β2) and six α-helices (α1–α6). All previously reported missense mutations are confined between α1 and α3 helices (i.e. mutational hotspot; Fig. 2A). L16P (between β1 and β2), F20S (β2), and R133Q (α6) are the first mutations that are located outside this hotspot. These data imply the importance of the β-turns and α6-helix of PAX8 in target DNA binding. As for the latter type, the D46fs mutation lacks 90% of normal protein sequence and acquires extra 23 frameshifted sequence. The results of western blotting with use of MG132 implied that the mutant was degraded via the proteasome-dependent pathway. Considering that the D46fs mutant consists of about 30% abnormal protein sequence, we speculate that the mutant was misfolded and was subject to endoplasmic reticulum-associated degradation. The D46fs mutation showed abrogated transactivation on the *TG* promoter irrespective of experimental conditions, supporting that it is actually a 'null' mutation. Our clinical and molecular data clearly demonstrate that one 'null'

PAX8 allele is enough to cause CH in humans (i.e. haploinsufficiency).

L16P, F20S, and R133Q had negligible transactivating capacities on the *TG* promoter in the TTF1 absent condition but showed significant transactivation when TTF1 is coexpressed. This 'rescue', which has been observed in three mutant PAX8 (S48F (11), H55Q (13), and K80_A84dup (12)) and one mutant TTF1 (P210L (19)), is likely based on the formation of PAX8–TTF1 complex on the *TG* promoter (20). However, no previous reports have tested whether those mutants could form the transcriptional complex. We suppose that demonstration of formation of the transcriptional complex containing the mutants, such as co-immunoprecipitation studies, will be required to verify the model.

In conclusion, we report clinical and molecular findings of four novel *PAX8* mutations, including three missense mutations located outside the previously recognized mutational hotspot and the first experimentally confirmed mutation with protein instability (D46fs). Our data imply that *PAX8* haploinsufficiency is enough to cause CH in humans.

Supplementary data

This is linked to the online version of the paper at http://dx.doi.org/10.1530/EJE-12-0410.

Declaration of interest

The authors declare that there is no conflict of interest that could be perceived as prejudicing the impartiality of the research reported.

Funding

The present work was supported by a Grant-in-Aid for Young Scientists (B) (24791087) from the Japan Society for the Promotion of Science (JSPS), a Grant-in-Aid for Scientific Research (C) (23591517) from JSPS, and the Health Science Research Grant for Research on Applying Health Technology (Jitsuyoka (Nanbyo)-Ippan-014) from the Ministry of Health, Labour and Welfare, Japan.

Acknowledgements

The authors would like to thank Prof. Takao Takahashi for fruitful discussion.

References

1 Plachov D, Chowdhury K, Walther C, Simon D, Guenet JL & Gruss P. Pax8, a murine paired box gene expressed in the developing excretory system and thyroid gland. *Development* 1990 **110** 643–651.

2 Zannini M, Francis-Lang H, Plachov D & Di Lauro R. Pax-8, a paired domain-containing protein, binds to a sequence overlapping the recognition site of a homeodomain and activates transcription from two thyroid-specific promoters. *Molecular and Cellular Biology* 1992 **12** 4230–4241. (doi:10.1128/MCB.12.9.4230)

3 Mansouri A, Chowdhury K & Gruss P. Follicular cells of the thyroid gland require Pax8 gene function. *Nature Genetics* 1998 **19** 87–90. (doi:10.1038/ng0598-87)

4 Congdon T, Nguyen LQ, Nogueira CR, Habiby RL, Medeiros-Neto G & Kopp P. A novel mutation (Q40P) in PAX8 associated with congenital hypothyroidism and thyroid hypoplasia: evidence for phenotypic variability in mother and child. *Journal of Clinical Endocrinology and Metabolism* 2001 **86** 3962–3967. (doi:10.1210/jc.86.8.3962)

5 de Sanctis L, Corrias A, Romagnolo D, Di Palma T, Biava A, Borgarello G, Gianino P, Silvestro L, Zannini M & Dianzani I. Familial PAX8 small deletion (c.989_992delACCC) associated with extreme phenotype variability. *Journal of Clinical Endocrinology and Metabolism* 2004 **89** 5669–5674. (doi:10.1210/jc.2004-0398)

6 Komatsu M, Takahashi T, Takahashi I, Nakamura M, Takahashi I & Takada G. Thyroid dysgenesis caused by PAX8 mutation: the hypermutability with CpG dinucleotides at codon 31. *Journal of Pediatrics* 2001 **139** 597–599. (doi:10.1067/mpd.2001.117071)

7 Macchia PE, Lapi P, Krude H, Pirro MT, Missero C, Chiovato L, Souabni A, Baserga M, Tassi V, Pinchera A, Fenzi G, Gruters A, Busslinger M & Di Lauro R. PAX8 mutations associated with congenital hypothyroidism caused by thyroid dysgenesis. *Nature Genetics* 1998 **19** 83–86. (doi:10.1038/ng0598-83)

8 Meeus L, Gilbert B, Rydlewski C, Parma J, Roussie AL, Abramowicz M, Vilain C, Christophe D, Costagliola S & Vassart G. Characterization of a novel loss of function mutation of PAX8 in a familial case of congenital hypothyroidism with in-place, normal-sized thyroid. *Journal of Clinical Endocrinology and Metabolism* 2004 **89** 4285–4291. (doi:10.1210/jc.2004-0166)

9 Vilain C, Rydlewski C, Duprez L, Heinrichs C, Abramowicz M, Malvaux P, Renneboog B, Parma J, Costagliola S & Vassart G. Autosomal dominant transmission of congenital thyroid hypoplasia due to loss-of-function mutation of PAX8. *Journal of Clinical Endocrinology and Metabolism* 2001 **86** 234–238. (doi:10.1210/jc.86.1.234)

10 Al Taji E, Biebermann H, Limanova Z, Hnikova O, Zikmund J, Dame C, Gruters A, Lebl J & Krude H. Screening for mutations in transcription factors in a Czech cohort of 170 patients with congenital and early-onset hypothyroidism: identification of a novel PAX8 mutation in dominantly inherited early-onset non-autoimmune hypothyroidism. *European Journal of Endocrinology* 2007 **156** 521–529. (doi:10.1530/EJE-06-0709)

11 Grasberger H, Ringkananont U, Lefrancois P, Abramowicz M, Vassart G & Refetoff S. Thyroid transcription factor 1 rescues PAX8/p300 synergism impaired by a natural PAX8 paired domain mutation with dominant negative activity. *Molecular Endocrinology* 2005 **19** 1779–1791. (doi:10.1210/me.2004-0426)

12 Narumi S, Muroya K, Asakura Y, Adachi M & Hasegawa T. Transcription factor mutations and congenital hypothyroidism: systematic genetic screening of a population-based cohort of Japanese patients. *Journal of Clinical Endocrinology and Metabolism* 2010 **95** 1981–1985. (doi:10.1210/jc.2009-2373)

13 Di Palma T, Zampella E, Filippone MG, Macchia PE, Ris-Stalpers C, de Vroede M & Zannini M. Characterization of a novel loss-of-function mutation of PAX8 associated with congenital hypothyroidism. *Clinical Endocrinology* 2010 **73** 808–814. (doi:10.1111/j.1365-2265.2010.03851.x)

14 Jo W, Ishizu K, Fujieda K & Tajima T. Congenital hypothyroidism caused by a PAX8 gene mutation manifested as sodium/iodide symporter gene defect. *Journal of Thyroid Research* 2010 **2010** 619013. (doi:10.4061/2010/619013)

15 Amendola E, De Luca P, Macchia PE, Terracciano D, Rosica A, Chiappetta G, Kimura S, Mansouri A, Affuso A, Arra C, Macchia V, Di Lauro R & De Felice M. A mouse model demonstrates a multigenic origin of congenital hypothyroidism. *Endocrinology* 2005 **146** 5038–5047. (doi:10.1210/en.2005-0882)

16 Yasumoto M, Inoue H, Ohashi I, Shibuya H & Onishi T. Simple new technique for sonographic measurement of the thyroid in neonates and small children. *Journal of Clinical Ultrasound* 2004 **32** 82–85. (doi:10.1002/jcu.10234)

17 Miccadei S, De Leo R, Zammarchi E, Natali PG & Civitareale D. The synergistic activity of thyroid transcription factor 1 and Pax 8 relies on the promoter/enhancer interplay. *Molecular Endocrinology* 2002 **16** 837–846. (doi:10.1210/me.16.4.837)

18 Narumi S, Yoshida A, Muroya K, Asakura Y, Adachi M, Fukuzawa R, Kameyama K & Hasegawa T. PAX8 mutation disturbing thyroid follicular growth: a case report. *Journal of Clinical Endocrinology and Metabolism* 2011 **96** E2039–E2044. (doi:10.1210/jc.2011-1114)

19 Carre A, Szinnai G, Castanet M, Sura-Trueba S, Tron E, Broutin-L'Hermite I, Barat P, Goizet C, Lacombe D, Moutard ML, Raybaud C, Raynaud-Ravni C, Romana S, Ythier H, Leger J & Polak M. Five new TTF1/NKX2.1 mutations in brain–lung–thyroid syndrome: rescue by PAX8 synergism in one case. *Human Molecular Genetics* 2009 **18** 2266–2276. (doi:10.1093/hmg/ddp162)

20 Di Palma T, Nitsch R, Mascia A, Nitsch L, Di Lauro R & Zannini M. The paired domain-containing factor Pax8 and the homeodomain-containing factor TTF-1 directly interact and synergistically activate transcription. *Journal of Biological Chemistry* 2003 **278** 3395–3402. (doi:10.1074/jbc.M205977200)

Received 10 May 2012
Revised version received 18 July 2012
Accepted 16 August 2012

OPEN ACCESS Freely available online

PLOS ONE

Gradual Loss of ACTH Due to a Novel Mutation in *LHX4*: Comprehensive Mutation Screening in Japanese Patients with Congenital Hypopituitarism

Masaki Takagi[1,2], Tomohiro Ishii[1], Mikako Inokuchi[1], Naoko Amano[1], Satoshi Narumi[1], Yumi Asakura[3], Koji Muroya[3], Yukihiro Hasegawa[2], Masanori Adachi[3], Tomonobu Hasegawa[1]*

1 Department of Pediatrics, Keio University School of Medicine Tokyo, Japan, **2** Department of Endocrinology and Metabolism, Tokyo Metropolitan Children's Medical Center, Tokyo, Japan, **3** Department of Endocrinology and Metabolism, Kanagawa Children's Medical Center, Kanagawa, Japan

Abstract

Mutations in transcription factors genes, which are well regulated spatially and temporally in the pituitary gland, result in congenital hypopituitarism (CH) in humans. The prevalence of CH attributable to transcription factor mutations appears to be rare and varies among populations. This study aimed to define the prevalence of CH in terms of nine CH-associated genes among Japanese patients. We enrolled 91 Japanese CH patients for DNA sequencing of *POU1F1, PROP1, HESX1, LHX3, LHX4, SOX2, SOX3, OTX2,* and *GLI2*. Additionally, gene copy numbers for *POU1F1, PROP1, HESX1, LHX3,* and *LHX4* were examined by multiplex ligation-dependent probe amplification. The gene regulatory properties of mutant LHX4 proteins were characterized *in vitro*. We identified two novel heterozygous *LHX4* mutations, namely c.249-1G>A, p.V75I, and one common *POU1F1* mutation, p.R271W. The patient harboring the c.249-1G>A mutation exhibited isolated growth hormone deficiency at diagnosis and a gradual loss of ACTH, whereas the patient with the p.V75I mutation exhibited multiple pituitary hormone deficiency. *In vitro* experiments showed that both *LHX4* mutations were associated with an impairment of the transactivation capacities of *POU1F1* and*αGSU*, without any dominant-negative effects. The total mutation prevalence in Japanese CH patients was 3.3%. This study is the first to describe, a gradual loss of ACTH in a patient carrying an *LHX4* mutation. Careful monitoring of hypothalamic–pituitary -adrenal function is recommended for CH patients with *LHX4* mutations.

Citation: Takagi M, Ishii T, Inokuchi M, Amano N, Narumi S, et al. (2012) Gradual Loss of ACTH Due to a Novel Mutation in *LHX4*: Comprehensive Mutation Screening in Japanese Patients with Congenital Hypopituitarism. PLoS ONE 7(9): e46008. doi:10.1371/journal.pone.0046008

Editor: Jean-Marc A Lobaccaro, Clermont Université, France

Received May 9, 2012; **Accepted** August 23, 2012; **Published** September 24, 2012

Copyright: © 2012 Takagi et al. This is an open-access article distributed under the terms of the Creative Commons Attribution License, which permits unrestricted use, distribution, and reproduction in any medium, provided the original author and source are credited.

Funding: This work was supported by Health and Labour Sciences Research Grant for Research on Applying Health Technology (Jitsuyoka (Nanbyo) - Ippan - 014). This work was supported by a grant from the Foundation for Growth Science, Japan. The funders had no role in study design, data collection and analysis, decision to publish, or preparation of the manuscript.

Competing Interests: The authors have declared that no competing interests exist.

* E-mail: thaseg@a6.keio.jp

Introduction

The proliferation and terminal differentiation of the anterior pituitary gland is strongly influenced by the precise spatial and temporal expression of transcription factors [1–3]. Mutations in these transcription factors often result in various types of congenital hypopituitarism (CH) [1–3]. Although previous studies have shown that these transcriptional factor mutations are rare among CH patients and that the mutation prevalence varies among populations, only a few genetic screening studies have been conducted. Graaff *et al.* identified a single patient with a *POU1F1* mutation from a study population of 79 multiple pituitary hormone deficiency (MPHD) patients (1.2%) in The Netherlands [4], and Dateki *et al.* reported one patient harboring an *LHX4* gross deletion from a cohort of 71 MPHD patients (1.4%) in Japan [5]. On the other hand, Reynaud *et al.* reported a mutation prevalence of 13.3% in a study population of 165 MPHD patients from the international GENHYPOPIT network [6]. Approximately 90% of the mutations identified in this report were *PROP1* common mutations (149delGA and 296delGA). Although the 296delGA mutation represents a mutational hot spot within the *PROP1* gene rather than a common founder mutation [7], studies from other ethnic groups often report a low prevalence of *PROP1* mutations [8,9].

This study aimed to determine the prevalence of transcription factor mutations in Japanese CH patients with PCR-based sequencing of nine CH-associated genes, namely *POU1F1, PROP1, HESX1, LHX3, LHX4, SOX2, SOX3, OTX2,* and *GLI2*. Additionally, we examined the gene copy numbers of *POU1F1, PROP1, HESX1, LHX3,* and *LHX4* by multiplex ligation-dependent probe amplification (MLPA).

Materials and Methods

Subjects

This study population consisted of 91 patients with GH-treated CH. The inclusion criteria were as follows: 1) short statue with severe GH deficiency (GH peak < 3 ng/mL) confirmed by hypoglycemic provocation test, and 2) anterior pituitary hypoplasia as detected by brain magnetic resonance imaging (MRI). We excluded any CH patients of known cause, such as a brain tumor or brain surgery from this study. Patients or parents of patients under 18 years of age gave their written informed consent to

Table 1. Endocrine phenotype of 91 probands screened for 9 genes.

	No. (%) with deficiencies of			
	GH	TSH	ACTH	LH/FSH
IGHD (n = 14)	14(100)			
MPHD (n = 77)	77(100)	61(79)	34(44)	19(24)

doi:10.1371/journal.pone.0046008.t001

participate in this study, which was approved by the Institutional Review Board of Keio University School of Medicine and the Institutional Review Board of Kanagawa Children's Medical Center.

Endocrinological investigations

Hormonal assays were performed using several commercial RIA kits, and normal values for each center were taken into account. The results of biochemical investigations at diagnosis were recorded including basal free thyroxine (fT4), TSH, cortisol and ACTH levels, their peaks in response to pituitary stimulation tests. The patients were evaluated for serum GH level after two consecutive classical provocative tests (with arginine or insulin). GH peaks <6 ng/mL after stimuli support a diagnosis of GHD. GH peak < 3 ng/mL by hypoglycemic provocation test define severe GHD. A diagnosis of TSH deficiency was made if serum fT4 concentration was under the normal level (fT4 < 1.0 ng/dL) with inadequate low serum TSH concentration. Cortisol peaks <17 μg/dL by hypoglycemic provocation tests define ACTH deficiency. FSH–LH deficiency was diagnosed on the basis of delayed or absent pubertal development and inadequate increase in serum FSH and LH in response to LHRH.

Imaging investigations

MRI included T1 and T2 weighted high-resolution pituitary imaging through the hypothalamo-pituitary axis (T1 sagittal 3-mm slices, T1 and T2 coronal 3-mm slices). Details noted included the size of the anterior pituitary, position of the posterior pituitary signal, presence and morphology of the optic nerves, optic chiasm, pituitary stalk, septum pellucidum, and corpus callosum.

Mutation screening

For all patients, regardless the phenotype/pituitary MRI findings, we analyzed all coding exons and flanking introns of *POU1F1*, *PROP1*, *HESX1*, *LHX3*, *LHX4*, *OTX2*, *SOX2*, *SOX3*, and *GLI2* by PCR-based sequencing. We screened for deletion/duplication involving *POU1F1*, *PROP1*, *HESX1*, *LHX3*, and *LHX4* by MLPA analyses (SALSA MLPA KIT P216; MRC-Holland, Amsterdam, The Netherlands). We tested any detected sequence variations against 150 Japanese control subjects.

RT-PCR

For mRNA analysis of the *LHX4* c.249-1G>A mutation, total RNA was extracted from Epstein-Barr virus-transformed lymphocytes derived from the propositus of pedigree 1. The cDNA produced from reverse transcription of RNA was subjected to PCR amplification using primers encompassing exons 2 to 4, and were subsequently processed for direct sequencing.

Functional studies

We performed functional studies on the two novel *LHX4* mutations (p.R84X and p.V75I). To generate LHX4 expression vectors, LHX4 cDNA was cloned into pCMV-myc and pEGFP-N1 (Clontech, Palo Alto, CA). We introduced the two mutations by site-directed mutagenesis, using the PrimeSTAR Mutagenesis Basal Kit (TaKaRa, Otsu, Japan). The luciferase reporter vectors were constructed by inserting the promoter sequences of *POU1F1* (*PIT1*),*αGSU* into a pGL3 basic vector (Promega, Madison, WI). A transactivation assay was performed using dual-luciferase reporter assay system (Promega) on COS7 and GH3 cells. For western blot analyses, we harvested COS7 cells transfected with the myc-tagged LHX4. Western blotting was performed with a mouse anti-myc monoclonal antibody (Invitrogen, Carlsbad, CA). For subcellular localization analyses, we visualized and photographed COS7 cells transfected with GFP-tagged LHX4 using a Leica TCS-SP5 laser scanning confocal microscope (Leica, Exton, PA). The sequences of the biotin-labeled doublestranded oligonucleotide used as probe in the EMSA experiment was 5′-GTATGAATCATTAATTGA-CAACATATTTTC-3′, as described previously [10]. The probes were detected with the Lightshift chemiluminescent EMSA kit (Pierce) according to the manufacturer's instruction.

Results

Patient details

Of the 91 patients, on the basis of hormonal deficiencies, 14 were determined to have isolated GH deficiency (IGHD), whereas 77 were MPHD. Detailed endocrine phenotype was available in all of the 91patients (Table 1). Results of the MRI scans were available in all patients with IGHD and MPHD. Details regarding the structural abnormalities of the hypothalamo-pituitary axis on neuroimaging in the probands are shown in Table 2. Among 77 MPHD patients, 12 were diagnosed as Septo-optic dysplasia.

Mutation screening

We identified two novel heterozygous *LHX4* mutations, namely c.249-1G>A, expected to cause exon skipping, and c.223G>A (p.V75I), and one common heterozygous *POU1F1* mutation,

Table 2. Results of MR scans of probands screened for 9 genes.

	Morphology of						
	Anterior pituitary	Posterior pituitary			Stalk		
	Hypoplasia	Normal	Ectopic	Absent	Normal	Invisible	Thin
IGHD (n = 14)	14	5	9	0	4	5	5
MPHD (n = 77)	77	24	51	2	23	25	29
Total (n = 91)	91	29	60	2	27	30	34

doi:10.1371/journal.pone.0046008.t002

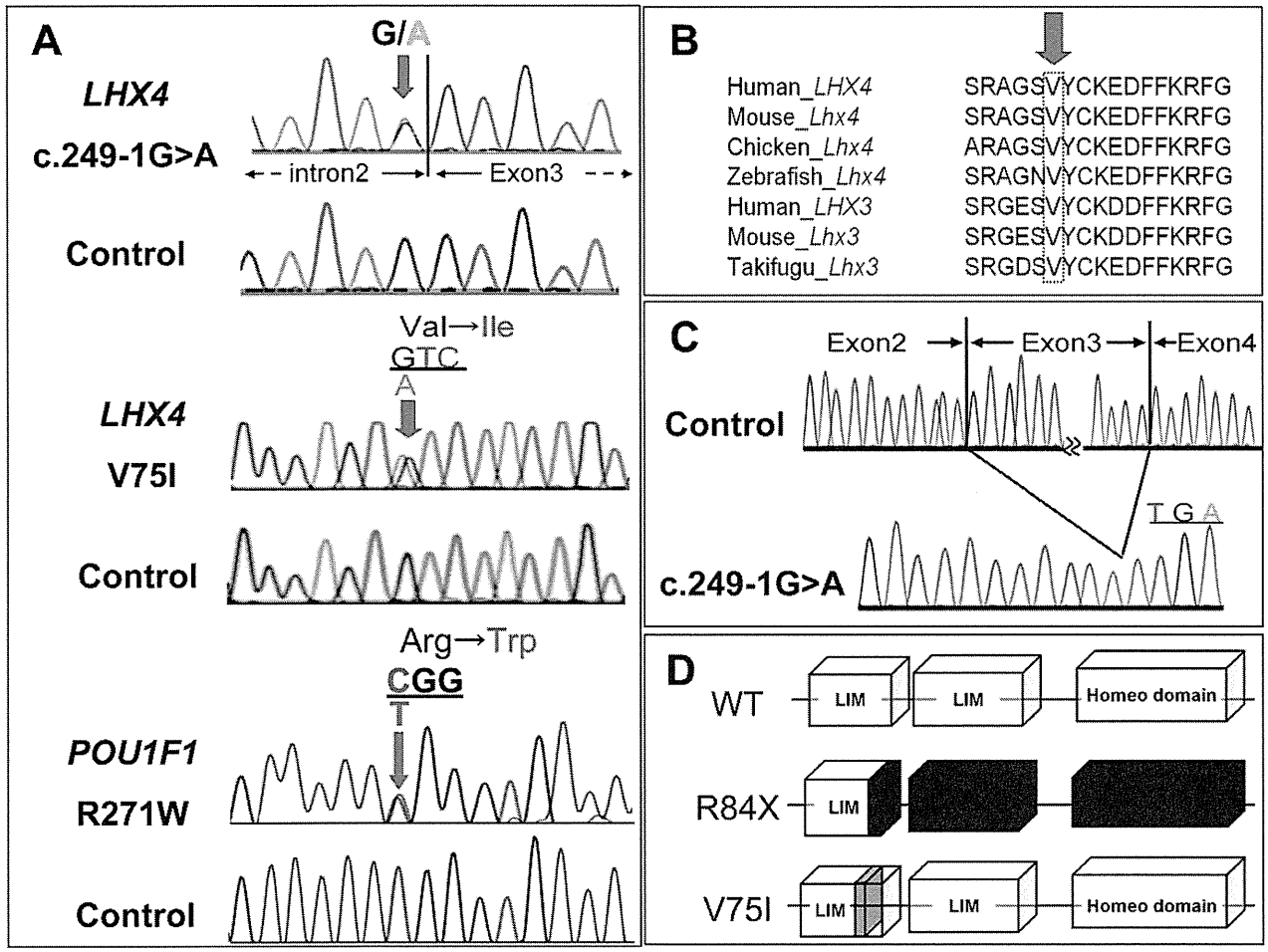

Figure 1. Identification of sequence variations of *LHX4* and *POU1F1*. *A*, Partial sequences of PCR products of the patients are shown. The upper chromatogram represents a heterozygous G to A substitution in the splice acceptor site of exon3. The middle chromatogram represents a heterozygous substitution of isoleucine (ATC) in place of valine (GTC) at codon 75. The arrow indicates the mutated nucleotide. The lower chromatogram represents a heterozygous substitution of tryptophan (TGG) in place of arginine (CGG) at codon 271. The arrow indicates the mutated nucleotide. *B*, Homology study showed valine at codon 75 is highly conserved through species in LHX4 and LHX3. C, Identification of exon3 skipping in the LHX4 cDNA derived from propositus of pedigree 1. LHX4 transcript with a deleted exon 3 creates a premature stop codon at the beginning of the remaining exon 4 (p.R84X). *D*, Schematic diagrams of the LHX4 protein. LHX4 cDNA encodes two LIM domains and one homeodomain. LHX4 with a p.R84X mutation results in the deletion of one of the two LIM domains and the entire homeodomain. Val75 is located within the first LIM domain.
doi:10.1371/journal.pone.0046008.g001

c.811C>T (p.R271W) [11] (FIG. 1A). The V75 in LHX4 is evolutionarily highly conserved (FIG. 1B), and these two *LHX4* mutations were not detected in any of the 150 healthy Japanese controls. We detected no gross or exon-level deletions/duplications using the MLPA analyses. For 14 IGHD patients, we additionally analyzed all coding exons and flanking introns of *GH1*, and *GHRHR* by PCR-based sequencing and MLPA (SALSA MLPA KIT P216 included all exons of *GH1* and *GHRHR*), failing to detect any sequence variation.

RT-PCR

The RT-PCR generated a product of smaller size than that obtained from a control sample. Sequencing revealed that it corresponded to a LHX4 transcript skipping exon 3 (FIG. 1C). If translated, this abnormal transcript would generate a protein lacking one of the two LIM domains (LD) and the entire homeodomain (HD), p.R84X (FIG. 1D).

Clinical phenotypes of the mutation carriers

Pedigree 1: *LHX4* c.249-1G>A (FIG. 2A). The propositus was a 16-year-old Japanese female, who was born at 39 weeks of gestation after an uncomplicated pregnancy and delivery. At birth, her length was 51.0 cm (1.2 SD) and weight 3.3 kg (0.6 SD). She was referred to us at 5 years of age because of short stature. Her height was 92.4 cm (-3.6 SD). Endocrine studies indicated that the patient had IGHD (Table 3). Brain MRI showed anterior pituitary hypoplasia, with a visible but thin stalk, and an ectopic posterior pituitary gland (EPP). No other central nervous system abnormalities were visualized. Recombinant human GH therapy was started at age 6. Her growth was responded well to GH replacement. Although she had no definite episode of adrenal insufficiency, longitudinal data showed that her blood cortisol peak, after stimulation by hypoglycemia with insulin tolerance tests, decreased gradually with age (20.5, 17.5, 16.4, and 10.0 μg/dL, at ages of 5, 13, 14, and 15 years, respectively, Ref. >17 μg/

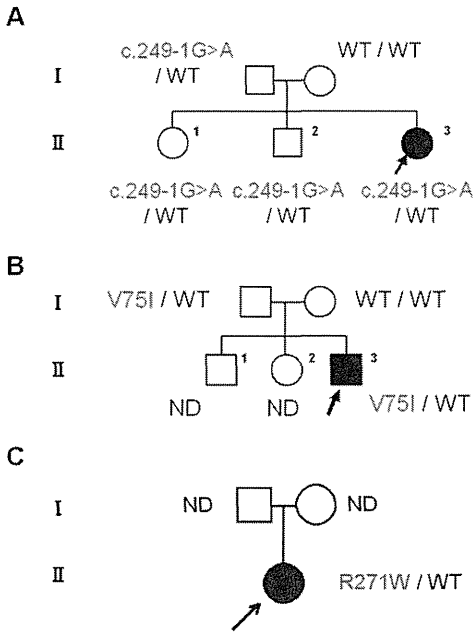

Figure 2. The pedigrees of the affected families. *A–C,* Pedigrees of families 1–3. Arrow indicates the propositus. ND: not determined.
doi:10.1371/journal.pone.0046008.g002

dL [12]), indicating of a gradual loss of ACTH. Follow-up MRI showed no changes as compared with the initial finding.

The father of the patient was 153.0 cm (-2.9 SD) tall, and the mother was 160.8 cm (0.5SD) tall. The elder brother and sister of the patient, both reached normal adult heights of 171.7 cm (0.2 SD) and 152.1 cm (-1.3 SD), respectively. Genetic analyses showed that the propositus, siblings and father carried the heterozygous *LHX4* c.249-1G>A mutation. No family members had any baseline hormonal abnormalities (Table 4).

Pedigree 2: *LHX4* p.V75I (FIG. 2B). The propositus was a 13-year-old Japanese male born at 41 weeks of gestation after an uncomplicated pregnancy and delivery. At birth, his length was 51.0 cm (1.0 SD) and weight 3.3 kg (0.7 SD). He was referred to us at 3 months of age because of a micropenis and bilateral cryptorchidism. He had undetectable plasma testosterone and LH levels, indicating hypogonadotropic hypogonadism. Severe growth failure was observed at the age of 11 months. Hormonal data revealed GH and TSH deficiencies in addition to tentative gonadotropin deficiency (Table 5). Brain MRI exhibited anterior pituitary hypoplasia, poorly developed sella turcica, visible but thin stalk, and EPP. No other central nervous system abnormalities were visualized. Replacement therapy with thyroxine and recombinant human GH was started at the age of 1 year. The patient responded well to GH replacement. At the age of 13 years, he showed small intrascrotal testes (1 ml), no pubic hair (P1), and a microphallus with low concentration of basal testosterone (0.05 ng/mL Ref: 2.0–7.5).

Table 3. Endocrinological findings in Propositus of pedigree 1.

		5yr			15yr			Reference	
	Stimulus	**Basal**		**Peak**	**Basal**		**Peak**	**Basal**	**Peak**
GH (ng/ml)	Insulin	2.7	→	2.9	1.8	→	2.6		>6
TSH (mIU/ml)	TRH	2.88	→	10.01	0.78	→	7.42		10–35
LH (mIU/ml)	LHRH	<0.2	→	2.8	6.7	→	21.2	<0.1[a]	1.93–4.73 [a]
								<0.10–2.65[b]	6.69–22.51 [b]
FSH (mIU/ml)	LHRH	0.5	→	15.5	7.0	→	9.6	0.64–3.03[a]	13.15–46.95[a]
								1.81–7.31[b]	8.58–17.62[b]
PRL (ng/ml)	TRH	10.4	→	19.7	5.7	→	28.1	1.7–15.4	increase 2 times
ACTH (pg/ml)	Insulin	44	→	46	7.3	→	14.9	9.8–27.3	28–130.5
Cortisol (μg/dl)	Insulin	19.1	→	20.5	7.5	→	10.0		>19.8[c]
									>17.0[d]
IGF-1 (ng/ml)		70.1			241			74–230[e]	
								262–510[f]	
Free T4 (ng/dl)		1.1			1.0			1.0–1.95	
Free T3 (pg/ml)		4.2			2.1			2.23–5.30	
Estradiol (pg/ml)					28			12.3–170[g]	

The conversion factors to the SI unit are as follows: GH 1.0 (μg/liter), LH 1.0 (IU/liter), FSH 1.0 (IU/liter), TSH 1.0 (mIU/liter), prolactin 1.0 (μg/liter), ACTH 0.22 (pmol/liter), cortisol 27.59 (nmol/liter), IGF-I 0.131 (nmol/liter), free T4 12.87 (pmol/liter), free T3, 1.54 (pmol/liter), and estradiol 3.671 (pmol/liter).
[a]Reference data of pre-pubertal Japanese girls [22]
[b]Reference data of pubertal (Tanner 2–3) Japanese girls [22]
[c]Reference data of UK children (younger than 10 years) [23]
[d]Reference data of UK children (older than 10 years) [23]
[e]Reference data of Japanese girls (5–7 years old) [24]
[f]Reference data of Japanese girls (15–17 years old) [24]
[g]Reference data of Japanese girls (15 years old) [25]
doi:10.1371/journal.pone.0046008.t003

Table 4. Endocrinological findings (baseline) in Family members of pedigree 1.

	Father	Mother	Brother	Sister	Reference (Adult)
GH (ng/ml)	0.7	3.2	0.5	0.4	0–23
IGF-1 (ng/ml)	110.0	156.0	357.0	276.0	Male: 41–369
					Female: 73–542
TSH (μU/ml)	0.77	1.60	0.50	0.94	0.3–3.50
Free T4 (ng/dl)	1.1	1.1	1.4	1.3	1.09–2.55
Free T3 (pg/ml)	2.5	2.6	3.1	3.1	3.23–5.11
LH (mIU/ml)	4.8	7.4	2.1	6.9	Male: 2.2–8.4
					Female: 1.4–15[a]
FSH (mIU/ml)	2.9	4.3	2.3	7.9	Male: 1.8–12
					Female: 3–10[a]
PRL (ng/ml)	11.2	11.2	7.8	5.5	Male: 1.5–9.7
					Female: 1.4–14.6
ACTH (pg/ml)	14	12	15	20	7.2–63.3
Cortisol (μg/dl)	8.2	6.3	10.3	10.3	7.6–21.4
Estradiol (pg/ml)		397		23	Female: 11–230[a]
Testosterone (ng/ml)	5.19		5.56		Male: 2.01–7.50

[a]Follicular phase

doi:10.1371/journal.pone.0046008.t004

The patient's father was 160.5 cm (-1.8 SD) tall. Genetic analyses showed that the propositus and father carried the same heterozygous *LHX4* p.V75I mutation. No other family member was available for genetic studies. Evaluation of the hormonal data for the father was refused.

Pedigree 3: *POU1F1* p.R271W (FIG. 2C). The propositus was a 28-year-old Japanese female, who was born at 37 weeks of gestation after an uncomplicated pregnancy and delivery. At birth, her length was 48.0 cm (-0.2 SD) and weight 2.6 kg (-1.0 SD). She was referred to us at 2 years of age because of severe short stature (-4.5 SD). Endocrine studies indicated that the patient had complete GH and PRL deficiencies and partial TSH deficiency (free T4 0.8 ng/dl, Ref. >1.0, with inadequate low TSH). Brain MRI at the age of 7 years exhibited anterior pituitary hypoplasia, normal stalk, and normal posterior pituitary gland. No other

Table 5. Endocrinological findings in Propositus of pedigree 2.

		11month			8yr			Reference	
	Stimulus	Basal		Peak	Basal		Peak	Basal	Peak
GH (ng/ml)	Insulin	1.1	→	0.9	0.6	→	0.6		>6
TSH (mIU/ml)	TRH	0.56	→	6.81	2.00	→	10.81		10-35
LH (mIU/ml)	LHRH	0.3	→	0.8	0.2	→	2.3	<0.1[a]	<0.10-4.29 [a]
FSH (mIU/ml)	LHRH	2.1	→	2.6	1.5	→	7.4	0.46-1.43[a]	5.38-11.67[a]
Testosterone (ng/ml)	HCG				<0.05		0.17		>1.2[a]
PRL (ng/ml)	TRH	5.6	→	10.1	7.7	→	13.0	1.7-15.4	increase 2 times
ACTH (pg/ml)	Insulin	44	→	170	44	→	50	9.8-27.3	28-130.5
Cortisol (μg/dl)	Insulin	31.0	→	38.4	13.4	→	17.2	5-20	>19.8[b]
IGF-1 (ng/ml)		6.9			157			18-150 [c]	
								50-356[d]	
Free T4 (ng/dl)		1.1			1.1			1.01-1.95	
Free T3 (pg/ml)		4.4			3.9			2.23-5.30	

The conversion factors to the SI unit are as follows: GH 1.0 (μg/liter), TSH 1.0 (mIU/liter), LH 1.0 (IU/liter), FSH 1.0 (IU/liter), testosterone, 0.035 (nmol/liter), prolactin 1.0 (μg/liter), ACTH 0.22 (pmol/liter), cortisol 27.59 (nmol/liter), IGF-I 0.131 (nmol/liter), free T4 12.87 (pmol/liter), and free T3, 1.54 (pmol/liter).

[a]Reference data of pre-pubertal Japanese boys (younger than 10 years) [22]

[b]Reference data of UK children (younger than 10 years) [23]

[c]Reference data of Japanese boys (younger than 1 years old) [24]

[d]Reference data of Japanese boys (7-9 years old) [24]

doi:10.1371/journal.pone.0046008.t005

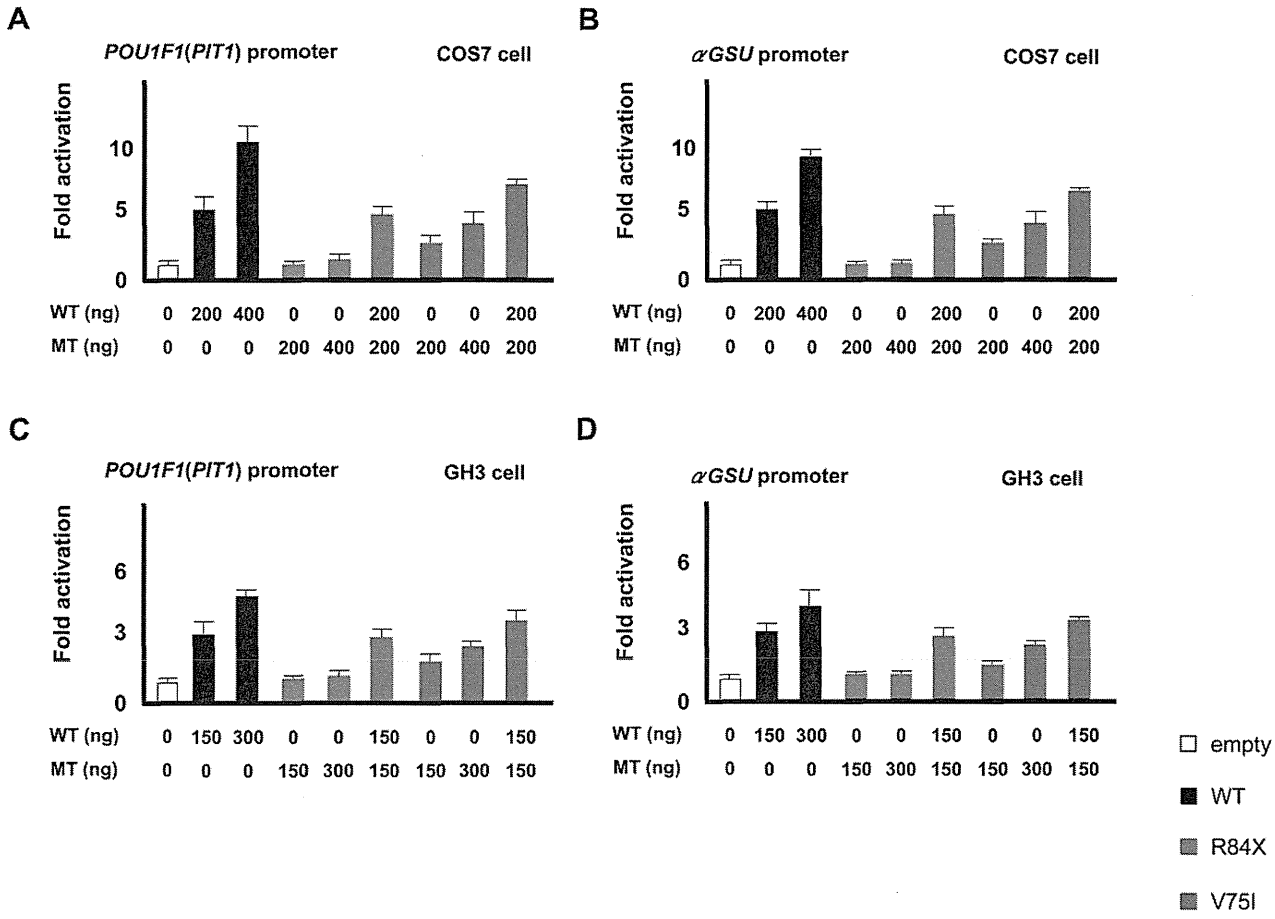

Figure 3. Transactivation assays of R84X and V75I LHX4 using *POU1F1*(*PIT1*) and*αGSU* reporter. *A and B*: COS7 cells were cotransfected with the pRL-CMV internal control vector, indicated amount (nanograms) of the effector plasmids, and the *POU1F1*(A) or*αGSU* (B) reporter. The data are the mean ± s.e.m. of at least three independent experiments performed in triplicate transfections. The white, black, red, and blue bars indicate the data of the empty expression vectors, expression vectors with wild type (WT) LHX4, expression vectors with R84X LHX4, and V75I LHX4, respectively. R84X LHX4 exhibited markedly reduced transactivation, whereas V75I LHX4 retained partial activity. The two mutants did not exhibit any dominant negative effect. The data are mean ± SEM of at least three independent experiments performed in triplicate transfections. *C and D*: GH3 cells were cotransfected with the pRL-CMV internal control vector, indicated amount (nanograms) of the effector plasmids, and the *POU1F1*(C) or*αGSU* (D) reporter.
doi:10.1371/journal.pone.0046008.g003

central nervous system abnormalities were visualized. The patient responded well to GH replacement.

Functional studies

Both in COS7 and GH3 cells, wild type LHX4 stimulated transcription of the *POU1F1* and*αGSU* reporters in a dose-dependent manner. R84X LHX4 had markedly reduced transactivation, whereas V75I LHX4 retained partial activity (FIG. 3A-D). The two mutants had no dominant negative effect. Western blot analysis showed that the expression of V75I LHX4 was comparable to that of the wild type, whereas R84X LHX4 was not detected (FIG. 4A). The V75I LHX4 mutant localized to the nucleus (FIG. 4B). WT LHX4 showed specific binding to the elements, which were competed by excess amount of (200 times) cold competitors. The V75I LHX4, which has an intact HD, bound with similar or slightly high efficiency to the WT LHX4 (FIG. 4C).

Discussion

In the present study, our mutation prevalence data (three mutation carriers in a total of 91 CH patients: 3.3%) is comparable with earlier report of Graaff *et al.* (1.2%) [4] or Dateki *et al* (1.4%) [5]. This study enrolled CH patients that fulfilled two definite inclusion criteria: 1) severe GH deficiency (GH peak < 3 ng/mL) confirmed by hypoglycemic provocation tests, which included IGHD and MPHD, and 2) anterior pituitary hypoplasia based on brain MRI. The subjects included in the two previous reports were diagnosed with MPHD and the reports of Dateki *et al.* did not describe any specific inclusion criteria. As *PROP1* common mutations (149delGA and 296delGA) are rare in Japan, our prevalence data were lower than that of Reynaud *et al.* [6]. These previous studies did not include screening for *SOX2*, *SOX3*, *OTX2* and *GLI2* (although the study by Dateki *et al.* included *SOX3* and *OTX2*), thus this study serves as the first report to include these genes. Despite extending the range of our genetic screening, our results imply the rarity of pathological abnormalities in the

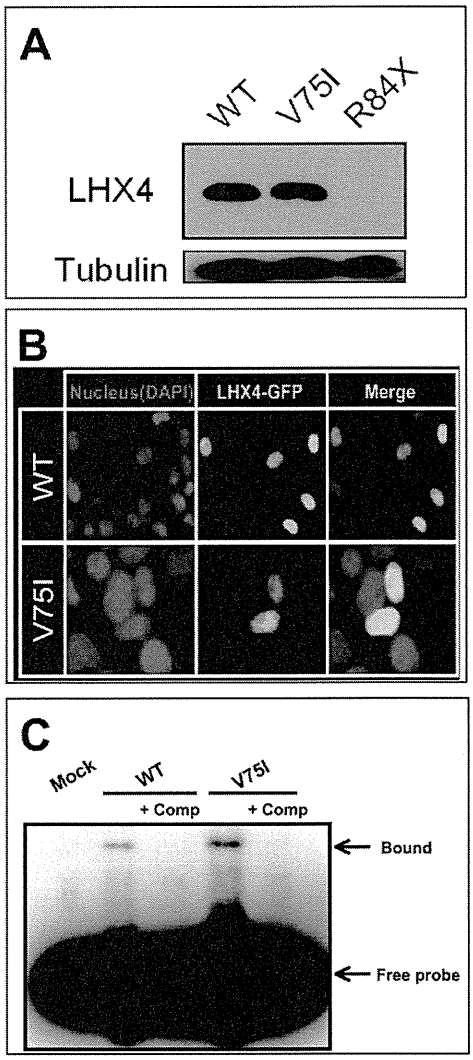

Figure 4. Functional characterization of two mutant LHX4. *A*, Protein expression level of myc-tagged WT and two LHX4 mutants was assessed by western blot using a monoclonal anti-myc antibody. The expression of V75I LHX4 was comparable to that of WT, whereas R84X LHX4 was not detected. Tubulin was used as a control. *B*, Subcellular localization analysis. For subcellular localization analyses, we visualized and photographed COS7 cells transfected with GFP-tagged LHX4 using a Leica TCS-SP5 laser scanning confocal microscope, after mounting the cells in Vectashield-DAPI solution. The WT and V75I LHX4 are localized to the nucleus. *C*, EMSA experiments. WT LHX4 showed specific binding to the elements, which was competed by excess amount of (200 times) cold competitors. The V75I LHX4, which has an intact HD, bound with similar or slightly high efficiency to the WT LHX4.
doi:10.1371/journal.pone.0046008.g004

currently known genes responsible for CH. Further studies are required to understand the pathogenesis of CH.

To date, eight families carrying a *LHX4* mutation have been reported [5,13–17]. We identified two novel mutations in *LHX4* (c.249-1G>A, p.V75I). Although both mutations were associated with impaired transactivation of *POU1F1* and*αGSU* without dominant-negative effects, indicating haploinsufficiency, the mechanism behind the loss of function resulting from these two mutations seems to be different. We did not detect R84X LHX4 on western blotting, indicating that the protein expression is markedly reduced due to the protein's instability. On the other hand, western blotting, visualization of subcellular localization, and DNA binding test revealed no significant difference between the wild type and V75I LHX4 variant. Val75 is a highly conserved amino acid located in the LD (FIG. 1C), which is important for protein-protein interaction, suggesting that substitution of Val75 to Ile results in defective interactions with transcriptional cofactors.

A striking finding of our report is that the propositus, who carried the c.249-1G>A *LHX4* mutation, exhibited a gradual loss of ACTH. Although late onset ACTH deficiency is well known in CH patients with *PROP1* mutations [18–20] and LHX3 [21], our study showed, for the first time, that a gradual loss of ACTH should be a point of concern among CH patients with *LHX4* mutations. Thus, this study suggests careful follow-up monitoring of the hypothalamic-pituitary-adrenal function in CH patients with *LHX4* mutations even if ACTH deficiency is not apparent at first evaluation. The patient's elder brother and sister were of normal adult height and had normal baseline hormonal levels. Even though this report is not the first description of the wide phenotypic spectrum in *LHX4* mutation carriers [13–17], it is noteworthy that *LHX4* mutation carriers can clinically and endocrinologically present as normal, even though the mutation is nonfunctional. The phenotypical variation documented in this study for patients with MPHD with mutations in *LHX4*, including dissimilarity within probands from the same pedigree, is likely partly due to the impact of other genes that are important but have not been recognized in pituitary development.

In summary, we found that only 3.3% of Japanese patients had mutation. *LHX4* mutation carriers exhibit wide phenotypic variability and can present as normal clinically and endocrinologically, even though they had a nonfunctional mutation. Gradual loss of ACTH should be monitored in CH patients with *LHX4* mutations.

Acknowledgments

We thank Kazue Kinoshita for technical assistance; Dr. Hirofumi Ohashi for establishing the Epstein-Barr virus transformed lymphocytes from the patient. We also thank Professor Takao Takahashi for his fruitful discussion of our study.

Author Contributions

Conceived and designed the experiments: MT SN TH. Performed the experiments: MT. Analyzed the data: MT. Contributed reagents/materials/analysis tools: TI MI NA SN YH YA KM MA. Wrote the paper: MT TH.

References

1. Romero CJ, Nesi-França S, Radovick S (2009) The molecular basis of hypopituitarism. Trends Endocrinol Metab 20:506–516.
2. Kelberman D, Rizzoti K, Lovell-Badge R, Robinson IC, Dattani MT (2009) Genetic regulation of pituitary gland development in human and mouse. Endocr Rev 30:790–829.
3. Pfäffle R, Klammt J (2011) Pituitary transcription factors in the aetiology of combined pituitary hormone deficiency. Best Pract Res Clin Endocrinol Metab 25:43–60.
4. de Graaff LC, Argente J, Veenma DC, Drent ML, Uitterlinden AG, et al. (2010) PROP1, HESX1, POU1F1, LHX3 and LHX4 mutation and deletion screening and GH1 P89L and IVS3+1/+2 mutation screening in a Dutch nationwide cohort of patients with combined pituitary hormone deficiency. Horm Res Paediatr 73:363–371.
5. Dateki S, Fukami M, Uematsu A, Kaji M, Iso M, et al. (2010) Mutation and gene copy number analyses of six pituitary transcription factor genes in 71

patients with combined pituitary hormone deficiency: identification of a single patient with LHX4 deletion. J Clin Endocrinol Metab 95:4043–4047.
6. Reynaud R, Gueydan M, Saveanu A, Vallette-Kasic S, Enjalbert A, et al. (2006) Genetic screening of combined pituitary hormone deficiency: experience in 195 patients. J Clin Endocrinol Metab 91:3329–3336.
7. Cogan JD, Wu W, Phillips JA 3rd, Arnhold IJ, Agapito A et al. (1998) The PROP1 2-base pair deletion is a common cause of combined pituitary hormone deficiency. J Clin Endocrinol Metab 83:3346–3349.
8. McLennan K, Jeske Y, Cotterill A, Cowley D, Penfold J, et al. (2003) Combined pituitary hormone deficiency in Australian children: clinical and genetic correlates. Clin Endocrinol 58:785–794.
9. Rainbow LA, Rees SA, Shaikh MG, Shaw NJ, Cole T, et al. (2005) Mutation analysis of POUF-1, PROP-1 and HESX-1 show low frequency of mutations in children with sporadic forms of combined pituitary hormone deficiency and septo-optic dysplasia. Clin Endocrinol (Oxf) 62:163–168.
10. Machinis K, Amselem S (2005) Functional relationship between LHX4 and POU1F1 in light of the LHX4 mutation identified in patients with pituitary defects. J Clin Endocrinol Metab 90: 5456–5462.
11. Radovick S, Nations M, Du Y, Berg LA, Weintraub BD, et al. (1992) A mutation in the POU-homeodomain of Pit-1 responsible for combined pituitary hormone deficiency. Science 257:1115–1118.
12. Crofton PM, Don-Wauchope AC, Bath LE, Kelnar CJ (2004) Cortisol responses to the insulin hypoglycaemia test in children. Horm Res 61:92–97.
13. Machinis K, Pantel J, Netchine I, Léger J, Camand OJ, et al. (2001) Syndromic short stature in patients with a germline mutation in the LIM homeobox LHX4. Am J Hum Genet 69:961–968.
14. Tajima T, Hattori T, Nakajima T, Okuhara K, Tsubaki J, et al. (2007) A novel missense mutation (P366T) of the LHX4 gene causes severe combined pituitary hormone deficiency with pituitary hypoplasia, ectopic posterior lobe and a poorly developed sella turcica. Endocr J 54:637–641.
15. Pfaeffle RW, Hunter CS, Savage JJ, Duran-Prado M, Mullen RD, et al. (2008) Three novel missense mutations within the LHX4 gene are associated with variable pituitary hormone deficiencies. J Clin Endocrinol Metab 93:1062–1071.
16. Castinetti F, Saveanu A, Reynaud R, Quentien MH, Buffin A, et al. (2008) A novel dysfunctional LHX4 mutation with high phenotypical variability in patients with hypopituitarism. J Clin Endocrinol Metab 93:2790–2799.
17. Tajima T, Yorifuji T, Ishizu K, Fujieda K (2010) A novel mutation (V101A) of the LHX4 gene in a Japanese patient with combined pituitary hormone deficiency. Exp Clin Endocrinol Diabetes 118: 405–409.
18. Mendonca BB, Osorio MG, Latronico AC, Estefan V, Lo LS, et al. (1999) Longitudinal hormonal and pituitary imaging changes in two females with combined pituitary hormone deficiency due to deletion of A301, G302 in the PROP1 gene. J Clin Endocrinol Metab 84:942–945.
19. Asteria C, Oliveira JH, Abucham J, Beck-Peccoz P (2000) Central hypocortisolism as part of combined pituitary hormone deficiency due to mutations of PROP-1 gene. Eur J Endocrinol 143:347–352.
20. Pernasetti F, Toledo SP, Vasilyev VV, Hayashida CY, Cogan JD, et al. (2000) Impaired adrenocorticotropin-adrenal axis in combined pituitary hormone deficiency caused by a two-base pair deletion (301-302delAG) in the prophet of Pit-1 gene. J Clin Endocrinol Metab 85:390–397.
21. Bonfig W, Krude H, Schmidt H (2011) A novel mutation of LHX3 is associated with combined pituitary hormone deficiency including ACTH deficiency, sensorineural hearing loss, and short neck-a case report and review of the literature. Eur J Pediatr 170:1017–1021.
22. Ito J, Tanaka T, Horikawa R, Okada Y, Morita S, et al. (1993) Serum LH and FSH levels during GnRH tests and sleep in children. J Jpn Pediatr Soc (in Japanese) 97:1789–1796.
23. Crofton PM, Don-Wauchope AC, Bath LE, Kelnar CJ (2004) Cortisol responses to the insulin hypoglycaemia test in children. Horm Res 61: 92–97.
24. Fujieda K, Shimazu A, Hanyuu K, Tanaka T, Yokoya S, et al. (1996) Clinical evaluation of serum IGF-I, IGF-II and IGFBP-3 measured by IRMA kits in childhood. Clinical Endocrinology (in Japanese) 44: 1229–1239.
25. Japan Public Health Association (1996) Normal biochemical values in Japanese children (in Japanese). Tokyo: Sanko Press.

OPEN ACCESS Freely available online

PLoS one

A Novel Mutation in *LEPRE1* That Eliminates Only the KDEL ER- Retrieval Sequence Causes Non-Lethal Osteogenesis Imperfecta

Masaki Takagi[1,2], Tomohiro Ishii[1], Aileen M. Barnes[3], MaryAnn Weis[4], Naoko Amano[1], Mamoru Tanaka[5], Ryuji Fukuzawa[6], Gen Nishimura[7], David R. Eyre[4], Joan C. Marini[3], Tomonobu Hasegawa[1]*

1 Department of Pediatrics, Keio University School of Medicine, Tokyo, Japan, **2** Department of Endocrinology and Metabolism, Tokyo Metropolitan Children's Medical Center, Tokyo, Japan, **3** Bone and Extracellular Matrix Branch, NICHD, NIH, Bethesda, Maryland, United States of America, **4** Orthopaedic Research Laboratories, University of Washington, Seattle, Washington, United States of America, **5** Department of Obstetrics and Gynecology, Keio University School of Medicine, Tokyo, Japan, **6** Department of Pathology and Laboratory Medicine, Tokyo Metropolitan Children's Medical Center, Tokyo, Japan, **7** Department of Radiology, Tokyo Metropolitan Children's Medical Center, Tokyo, Japan

Abstract

Prolyl 3-hydroxylase 1 (P3H1), encoded by the *LEPRE1* gene, forms a molecular complex with cartilage-associated protein (CRTAP) and cyclophilin B (encoded by *PPIB*) in the endoplasmic reticulum (ER). This complex is responsible for one step in collagen post-translational modification, the prolyl 3-hydroxylation of specific proline residues, specifically α1(I) Pro986. P3H1 provides the enzymatic activity of the complex and has a Lys-Asp-Glu-Leu (KDEL) ER-retrieval sequence at the carboxyl terminus. Loss of function mutations in *LEPRE1* lead to the Pro986 residue remaining unmodified and lead to slow folding and excessive helical post-translational modification of type I collagen, which is seen in both dominant and recessive osteogenesis imperfecta (OI). Here, we present the case of siblings with non-lethal OI due to novel compound heterozygous mutations in *LEPRE1* (c.484delG and c.2155dupC). The results of RNA analysis and real-time PCR suggest that mRNA with c.2155dupC escapes from nonsense-mediated RNA decay. Without the KDEL ER- retrieval sequence, the product of the c.2155dupC variant cannot be retained in the ER. This is the first report of a mutation in *LEPRE1* that eliminates only the KDEL ER-retrieval sequence, whereas other functional domains remain intact. Our study shows, for the first time, that the KDEL ER- retrieval sequence is essential for P3H1 functionality and that a defect in KDEL is sufficient for disease onset.

Citation: Takagi M, Ishii T, Barnes AM, Weis M, Amano N, et al. (2012) A Novel Mutation in *LEPRE1* That Eliminates Only the KDEL ER- Retrieval Sequence Causes Non-Lethal Osteogenesis Imperfecta. PLoS ONE 7(5): e36809. doi:10.1371/journal.pone.0036809

Editor: Eugene A. Permyakov, Russian Academy of Sciences, Institute for Biological Instrumentation, Russian Federation

Received December 10, 2011; **Accepted** April 6, 2012; **Published** May 15, 2012

Copyright: © 2012 Takagi et al. This is an open-access article distributed under the terms of the Creative Commons Attribution License, which permits unrestricted use, distribution, and reproduction in any medium, provided the original author and source are credited.

Funding: This work was supported by Research on Intractable Diseases of Health and Labour Sciences Research Grants (Diagnosis and treatment of osteogenesis imperfect; H22-Nanji-Ippan-194) from the Ministry of Health, Labour and Welfare of Japan, and by a grant from the Japan Society for the Promotion of Science (Grant-in-Aid for Young Scientists (B) (22790999)). The funders had no role in study design, data collection and analysis, decision to publish, or preparation of the manuscript.

Competing Interests: The authors have declared that no competing interests exist.

* E-mail: thaseg@a6.keio.jp

Introduction

Osteogenesis imperfecta (OI; MIM #166200, #166210, #259420, #166220, #610967, #610968, #610682, #610915, #259440, #613848 and #613982) comprises a heterogeneous group of connective tissue disorders characterized by fragile bones with susceptibility to fractures. Most cases of OI are caused by heterozygous mutations in *COL1A1* or *COL1A2*, the genes encoding the two type I procollagen alpha chains, proα1 (I) and proα2 (I) [1]. Mutations in these genes result in quantitative and/or qualitative defects in type I collagen production by osteoblasts [2–4].

Recurrence of severe OI in families with unaffected parents results from either dominant (parental mosaicism) or recessive inheritance [5–7]. Recent investigations have discovered several genes responsible for OI inherited as an autosomal recessive trait [8–18]. Among these genes, *LEPRE1* encodes prolyl 3-hydroxylase 1 (P3H1), which forms a molecular complex with cartilage-associated protein (CRTAP) and cyclophilin B (CypB, encoded by *PPIB*) in the endoplasmic reticulum (ER) that is responsible for one step in collagen post-translational modification, the prolyl 3-hydroxylation of specific proline residues, specifically α1(I) Pro986 [19]. P3H1 provides the enzymatic activity of the complex and is the only component of the complex with a Lys-Asp-Glu-Leu (KDEL) ER-retrieval sequence at the carboxyl terminus [20]. Loss of function mutations in either *LEPRE1* or *CRTAP* lead to loss of both proteins in the cell, leave the Pro986 residue unmodified, and lead to slow folding and excessive helical post-translational modification of type I collagen [21].

To date, more than 20 *LEPRE1* mutations have been described [10,21–25]. With the exception of only one missense mutation, Leu489Pro [25], all *LEPRE1* mutations result in a premature termination codon (PTC) with mRNA that is destroyed by the process of nonsense-mediated RNA decay. Here we present the case of siblings with OI due to novel compound heterozygous mutations in *LEPRE1* (c.484delG and c.2155dupC). Without the KDEL ER- retrieval sequence, the product of the c.2155dupC variant cannot be retained in the ER. Our study shows, for the first time, that the KDEL ER- retrieval sequence is essential for P3H1

functionality and that a defect in KDEL is sufficient for disease onset.

Results

Patient Reports

Patient II-2 was a 5-year-old female born to healthy parents who already had one healthy child (Fig 1A). Prenatal ultrasonography at 28 weeks of gestation showed deformity of the lower limbs. She was delivered with multiple fractures by caesarian section at 35 weeks' gestation. Birth weight was 1966 g (below 3rd percentile), length 42.2 cm (below 3rd percentile), and OFC 31.2 cm (3rd–10th percentile). She did not have blue sclera or dysmorphic facial features, such as micrognathia or a triangular face. She had no neonatal respiratory distress. Radiographs showed multiple rib fractures, healed fractures of both femora and the right humerus, and a subacute fracture of the left humerus (Fig 1B). Metaphyseal osteopenia was significant. A diagnosis of OI type III was made. At least 10 fractures occurred in the first 6 months of life. Pamidronate treatment was initiated at 2 months of age. The pamidronate was initially administered by infusion every 2 months and was changed to every 3 months at the age of 2 years. The bone mineral density (BMD) of the lumber spine (L2–L4) was 0.336 gm/cm^2 (Z score of –2.2), 0.429 g/cm^2 (Z score of –2.7), 0.479 g/cm^2 (Z score of –4.9), and 0.514 g/cm^2 (Z score of –5.9) at the ages of 1 year, 2 years, 4 years, and 5 years respectively (We used BMD reference data [26] in Spanish children). She did not have severe deformity of the long bones at age 5 years, and her skin was normal in extensibility. She had white sclerae and normal dentition. She was able to walk with difficulty while holding on to a table. Her intellectual development was normal.

Patient II-3 was the product of couple's next pregnancy; this pregnancy was electively terminated. Postmortem radiographs showed bilateral femoral bowing, a healed fracture of the right femoral shaft, thin ribs, and metaphyseal demineralization (Fig 1C).

Patient II-3 Bone Histology

Bone samples, obtained at autopsy, from Patient II-3 were processed according to standard procedure, and the formalin fixed paraffin-embedded sections were stained with hematoxylin and eosin. Irregular trabeculae of woven bone rimed by osteoblasts were observed in the humerus (Fig 1D) and spine (Fig 1E). The stroma surrounding the woven bone was mildly to moderately cellular and consisted of fibroblasts and collagen. These histological features resembled those of osteofibrous dysplasia.

Detection of *LEPRE1* Mutations

Sequence analysis revealed novel compound heterozygous *LEPRE1* mutations (c.484delG, p.A162LfsX22 and c.2155dupC, p.E719RfsX11) in both patients (Fig 2A). Their father carried c.484delG and their mother carried c.2155dupC. These mutations were not found in 200 control alleles. No sequence variation was found in *COL1A1*, *COL1A2*, *CRTAP*, or *PPIB*, and neither exon-level deletion nor duplication involving *COL1A1* and *COL1A2* was detected by MLPA analysis. The p.E719RfsX11 mutation creates a PTC in the last exon and results in the lack of only the KDEL ER-retrieval sequence, whereas other functional domains, such as the tetratricopeptide domain and Prolyl/Lysyl hydroxylase domain, remain intact (Fig 2B).

LEPRE1 Transcripts and P3H1 Protein in Probands

Only the allele with c.2155 dupC was successfully amplified and sequenced at the cDNA level.

Real-Time PCR revealed that the level of *LEPRE1* transcripts of Patient II-3 was about one-half the control level (Fig 3A).

Western blot analysis of fibroblast lysates confirmed the absence of intracellular P3H1 in Patient II-3 (Fig 3C). Fluorescent microscopy showed the expected colocalization of P3H1 and CRTAP with GRP94 in control cells. Both P3H1 and CRTAP proteins were absent in fibroblasts from Patient II-3 (Fig 3D), reflecting mutual protection in the complex.

Collagen Post-translational Modification

In both the cell layer and media, steady-state fibroblast collagen of Patient II-3 displayed helical overmodification, detected as back-streaking of collagen alpha chain bands on gel electrophoresis (Fig 3B).

Tandem mass spectrometry analysis of tryptic peptides of Patient II-3 secreted α1 (I)-collagen chains revealed only a slight reduction (85% in proband, 95–98% in control collagen) of Pro986 3-hydroxylation (data not shown) despite the absence of detectable mutant P3H1 protein in the cell.

Discussion

ER-resident proteins must be distinguished from newly synthesized secretory proteins, which pass through this compartment as they transit the secretory pathway toward the extracellular space. One of the mechanisms by which this is achieved is the selective retrograde transport of soluble ER-resident proteins from the cis-Golgi to the ER [27]. Receptors in post-ER compartments recognize a C-terminal motif that marks proteins that are to be retained in the ER. The KDEL motif binds to this salvaging receptor (KDEL receptor) in the Golgi, resulting in this ligand-receptor complex being returned to the ER [27]. Soluble ER-resident proteins such as molecular chaperones and components of the control quality machinery, e.g. immunoglobulin heavy-chain binding protein, calreticulin, and protein disulfide isomerase, contain the KDEL motif at the carboxyl terminus. P3H1, encoded by *LEPRE1*, forms a molecular complex with CRTAP and CypB in the ER, and provides the enzymatic activity of the complex. P3H1 is the only component of the complex with a KDEL ER-retrieval sequence at the carboxyl terminus [20]. One splice mutation, c.2055+18G>A, which abolishes the *LEPRE1* mRNA splice form of KDEL, has previously been reported [23]. This splice mutation results in preferential use of alternative splice donor site, and a significant decrease in the *LEPRE1* mRNA splice form containing the KDEL sequence. However, this finding does not provide direct evidence for the importance of the KDEL sequence. The case presented here is therefore the first report of a mutation in *LEPRE1* that eliminates only the KDEL ER-retrieval sequence, while all other functional domains remain intact. Without the KDEL ER- retrieval sequence, the c.2155dupC variant will not captured by KDEL receptor in the Golgi. Our report shows, for the first time, that the KDEL ER-retrieval sequence is essential for P3H1 functionality *in vivo*. Dysfunction of this KDEL-KDEL receptor interaction will provide us one disease causing mechanism of OI as well as other diseases involved in ER enzyme.

It is noteworthy that our proband's collagen contained higher percentage (85%) of 3-hydroxylated Pro986 residues than previously reported with *LEPRE1* null mutations, which showed severely reduced (0–15%) 3-hydroxylation of Pro986 [10,22,23]. We could not detect mutant P3H1 in the proband cells by western blotting assay or fluorescent microscopy. However, we hypothesize that the P3H1/CRTAP/CyPB complex that includes the mutant P3H1 without KDEL must be transiently present in the ER at

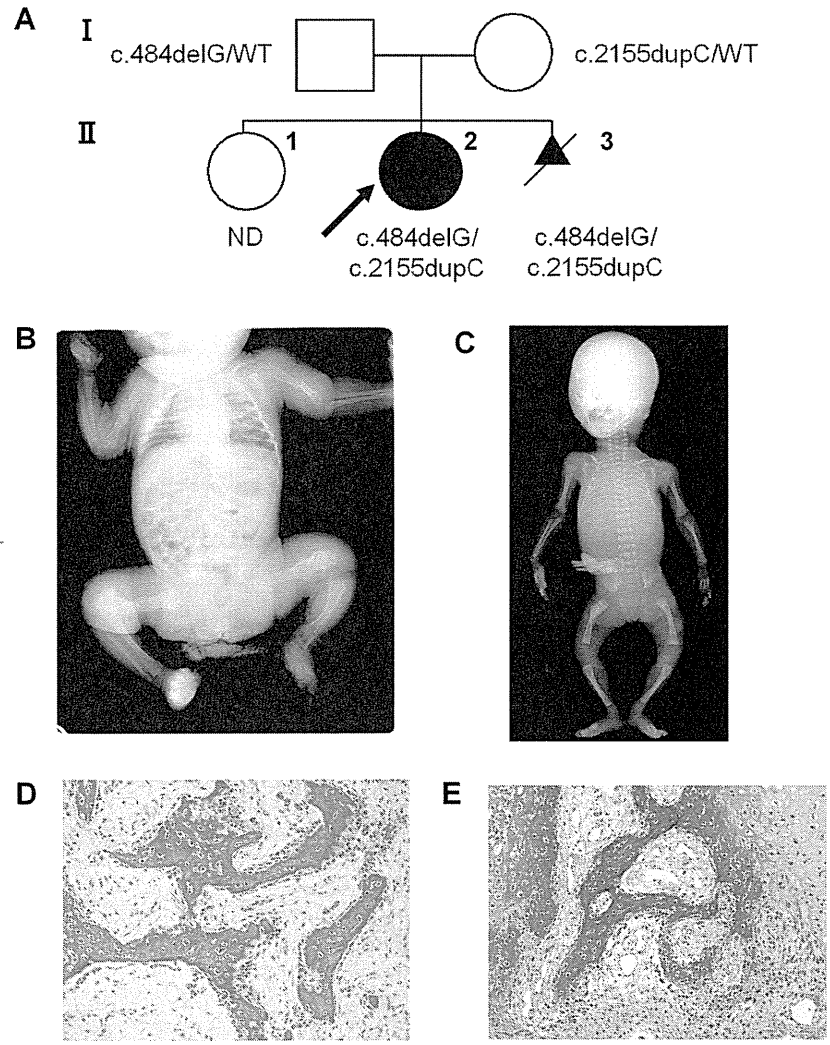

Figure 1. Features of Siblings with Mutations of *LEPRE1*. A: The pedigree of the affected family. The arrow indicates the proband. Patient II-3 was electively terminated. B: Radiographs of Patient II-2 as a neonate. There were multiple rib fractures, healed fractures of both femora and the right humerus, and a subacute fracture of the left humerus. Metaphyseal osteopenia was significant. C: Postmortem radiographs of Patient II-3. Bilateral femoral bowing, a healed fracture of the right femoral shaft, thin ribs, and metaphyseal demineralization were shown. D, E: Histological findings of Patient II-3. Irregular trabeculae of woven bones lined by osteoblasts are observed in the humerus (D) and spine (E). The stroma is cellular and consists of fibroblasts and collagen resembling osteofibrous dysplasia.
doi:10.1371/journal.pone.0036809.g001

some minimal level, which is sufficient for 3-hydroxylating most α1(I) Pro986 residues. Recently, it was reported that the P3H1/CRTAP/CyPB complex has 3 distinct activities: it is a prolyl 3-hydroxylase, a PPIase, and a molecular chaperone [28]. In the present patient, despite the higher percentage of 3-hydroxylated Pro986 residues, overmodification of the patient's type I collagen was observed electrophoretically. This observation implicates the dysfunctional P3H1/CRTAP/CyPB complex in the pathology, with potential roles for absence of its chaperone or PPIase functions. However, since our proband has generally milder OI than described for null *LEPRE1* mutations, the OI severity may correlate with the level of type I collagen P986 3-hydroxylation.

In conclusion, our study shows, for the first time, that the KDEL ER- retrieval sequence is important for P3H1 functionality *in vivo*. In addition, the higher percentage of 3-hydroxylated P986 residues seen in the collagen of our patient correlates with her moderate phenotype, in contrast to the severe/lethal OI of probands with null *LEPRE1* mutations and minimal collagen 3-hydroxylation.

Materials and Methods

PCR-Based Mutation Screening

Approval for this study was obtained from the Institutional Review Board of Keio University School of Medicine. The parents gave written informed consent for the molecular studies.

Genomic DNA was extracted from peripheral blood (Patient II-2) and blood of the umbilical cord (Patient II-3) by a standard technique. We analyzed all coding exons and flanking introns of *COL1A1, COL1A2, LEPRE1, CRTAP,* and *PPIB* by PCR and direct sequencing. Deletion or duplication involving *COL1A1* and *COL1A2* was checked by multiplex ligation-dependent probe amplification (MLPA) analyses (SALSA MLPA KIT P271, P272; MRC-Holland, Amsterdam, The Netherlands).

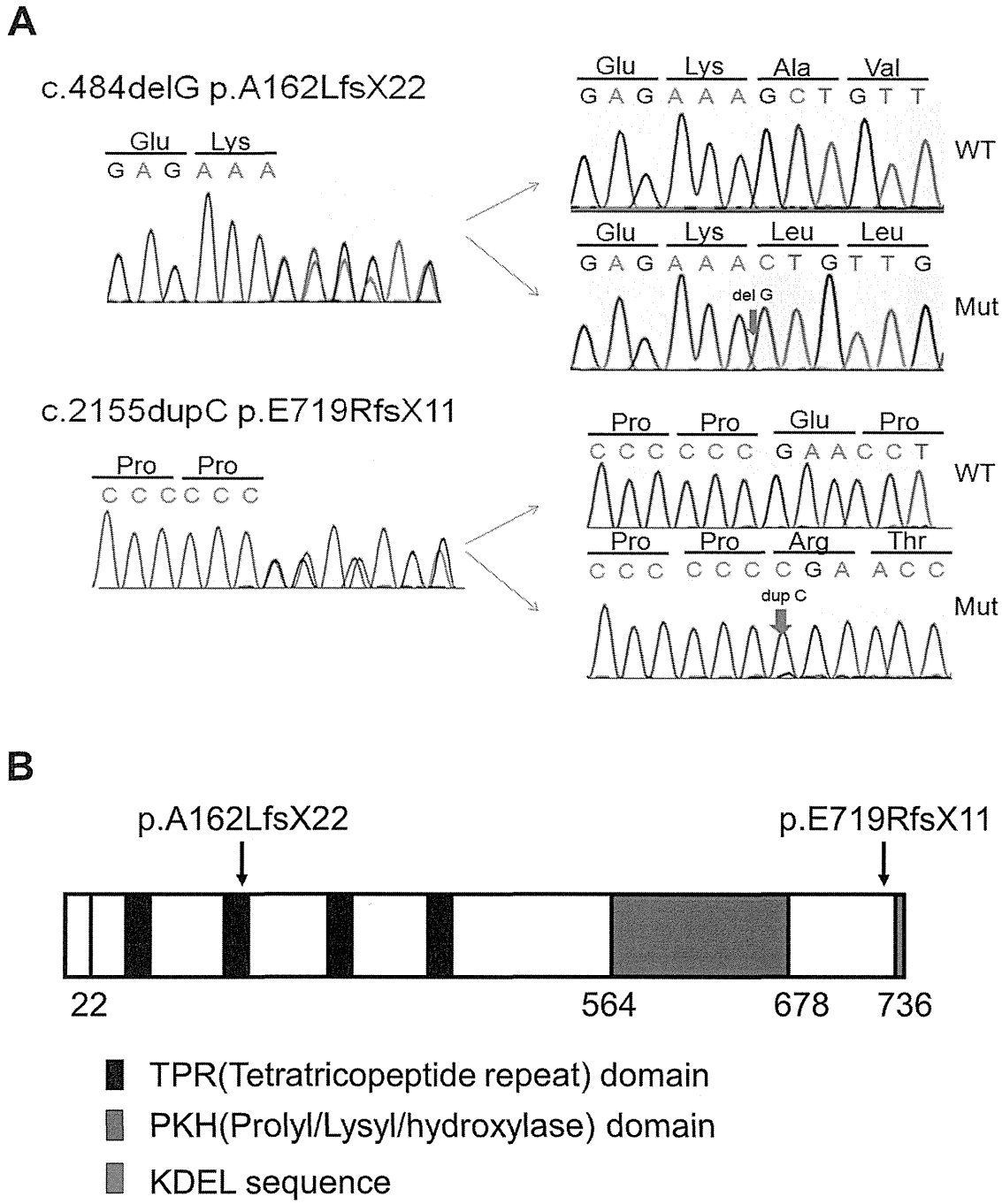

Figure 2. Identification of *LEPRE1* mutations. A: A partial sequence of PCR product of Patient II-3 is shown. Compound heterozygous frame shift mutations (c.484delG, p.A162LfsX22 and c.2155dupC, p.E719RfsX11) are indicated by arrows. The mutations have been confirmed by the subsequent sequencing of subcloned products of normal and mutant alleles. B: Schematic presentation of the positions of the mutation. *LEPRE1* cDNA encodes the tetratricopeptide repeat domain (four black regions), the Prolyl/Lysyl/hydroxylase domain (green region), and the KDEL ER- retrieval motif (red region). *LEPRE1* with a p.E719RfsX11 change results in the lack of only the KDEL ER-retrieval sequence, whereas other functional domains remain intact.
doi:10.1371/journal.pone.0036809.g002

RNA Analysis and Real-Time PCR

Total RNA was extracted from skin fibroblasts of Patient II-3 and cDNA synthesis was performed with the SuperScript III reverse transcriptase kit (Invitrogen, Carlsbad, CA) with oligoDT primers. Exons 2 and 15 of *LEPRE1* were amplified from cDNA by PCR. Subsequently, the PCR products were subjected to direct sequencing.

Real-time quantitative PCR was performed on the ABI PRISM 7500 Fast Real-Time PCR System (Applied Biosystems, Foster City, CA). For PCR reaction, we used SYBR Premix Ex Taq II

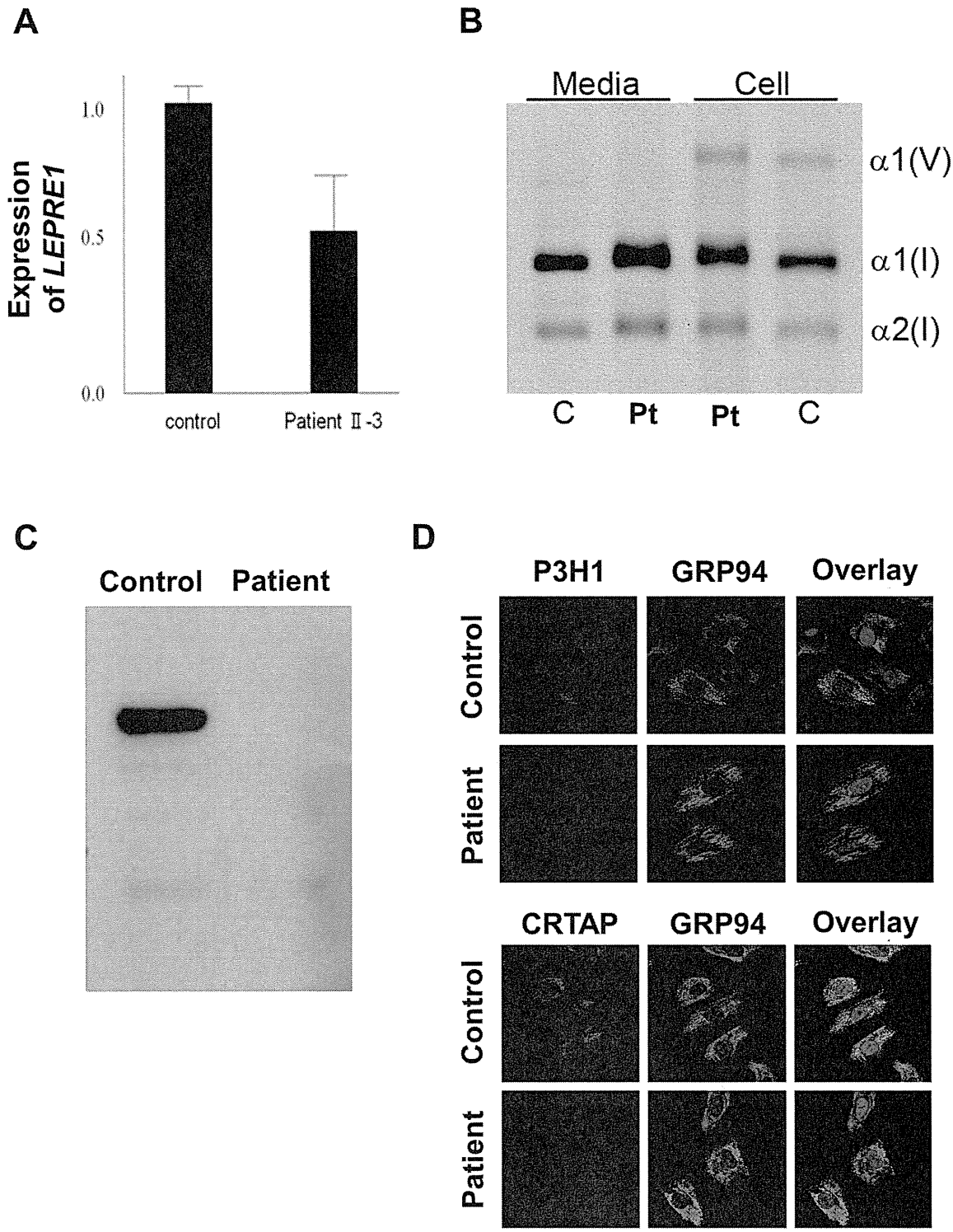

Figure 3. Characterization of the *LEPRE1* mutations and proband collagen. A: Patient II-3 *LEPRE1* transcripts are about one-half the control level, by real-time RT-PCR. B: Steady-state type I collagen protein from fibroblasts of Patient II-3 and a normal control is shown. In both the cell layer and media, overmodification, detected as back-streaking of collagen alpha chains (α1 (I) and α2 (I)) on gel electrophoresis, is present in Patient II-3. We also detected mild overmodification of type V collagen (α1 (V)). C: Western blots of fibroblast P3H1 in Patient II-3 and control cells confirm absence of intracellular P3H1. D: Immunofluorescent staining of fibroblasts from Patient II-3 and a normal control show colocalization of P3H1 and CRTAP with GRP94 in control cells. Both P3H1 and CRTAP proteins are absent in fibroblasts from Patient II-3.
doi:10.1371/journal.pone.0036809.g003

(Takara, Otsu, Japan). *LEPRE1* expression was calculated using a control fibroblast mRNA standard curve, then normalized to a constitutively expressed gene (b2-microglobulin). All reactions were carried out in triplicate and expression levels were determined in 3 independent experiments.

Western Blotting

Skin fibroblasts from Patient II-3 and a control subject were cultured in Dulbecco's modified Eagle's medium (DMEM) and were lysed in RIPA buffer (Sigma). Samples were subjected to 10% SDS-PAGE and then transferred onto polyvinylidene fluoride membrane. The membrane was treated with 10% milk powder solution overnight at 4°C, and incubated with primary antibody: mouse anti-LEPRE1 MaxPab polyclonal antibody (Abnova, Taipei, Taiwan) at a 1:1000 dilution. After washing, the membrane was incubated with secondary antibody: goat anti-mouse HRP conjugated (Invitrogen) at a 1:1000 dilution. The membrane was washed again and then scanned to visualize the specific protein band.

Steady-state Collagen Analysis

Control and Patient II-3 dermal fibroblasts were grown to confluence in DMEM + Glutamax^{TM} supplemented with 10% fetal bovine serum and penicillin/streptomycin. Cells were labeled overnight in serum-free medium containing 50 μg/ml ascorbic acid and 437.5 μCi/ml L-[2,3,4,5-^{3}H]proline. Collagens were precipitated with ammonium sulfate, pepsin-digested and separated on 6% SDS-Urea PAGE.

Immunocytochemistry

Immunofluorescence microscopy was performed as described [21]. Control and Patient II-3 dermal fibroblasts were grown on chamber slides. For CRTAP/GRP94 staining, cells were fixed in 4% paraformaldehyde, permeabilized with 0.1% TritonX-100 on ice, and blocked in 1% BSA in PBS. Cells were then incubated overnight with primary antibody (CRTAP, Abnova, Taipei, Taiwan; GRP94, Abcam, Cambridge, MA). After washing, cells were incubated with 1:200 Alexa Fluor secondary antibodies (Invitrogen) in blocking buffer for 1 h, washed, and mounted with coverslips. Cells were imaged using a Zeiss LSM 510 Inverted Meta microscope and LSM510 software. P3H1/GRP94 staining was done following the protocol of Willaert *et al* [23]. Cells were washed, then fixed and permeabilized in cold acetone. Cells were then blocked in 10% goat serum and incubated with primary antibody (LEPRE1 MaxPab, Abnova, Taipei, Taiwan) for 2.5 h. Secondary staining and imaging was done as above.

Tandem Mass Spectrometry

Secreted collagens from ascorbic acid stimulated fibroblast cultures were precipitated and the α1(I) bands were isolated and digested with trypsin. Electrospray mass spectrometry was performed as before [9].

Acknowledgments

We thank the patients and their families for participation in this study. We also thank Prof. Takao Takahashi for fruitful discussion. We would like to acknowledge the NICHD Microscopy and Imaging Core, in which the confocal microscopy was conducted.

Author Contributions

Conceived and designed the experiments: M. Takagi DRE JCM TH. Performed the experiments: M. Takagi AMB MW. Analyzed the data: M. Takagi AMB MW RF GN. Contributed reagents/materials/analysis tools: TI NA M. Tanaka. Wrote the paper: M. Takagi JCM TH.

References

1. Marini JC, Forlino A, Cabral WA, Barnes AM, San Antonio JD, et al. (2007) Consortium for osteogenesis imperfect mutations in the helical domain of type I collagen: regions rich in lethal mutations align with collagen binding sites for integrins and proteoglycans. Hum Mutat 28: 209–221.
2. Willing MC, Deschenes SP, Slayton RL, Roberts EJ (1996) Premature chain termination is a unifying mechanism for *COL1A1* null alleles in osteogenesis imperfecta type I cell strains. Am J Hum Genet 59: 799–809.
3. Körkkö J, Ala-Kokko L, De Paepe A, Nuytinck L, Earley J, et al. (1998) Analysis of the *COL1A1* and *COL1A2* genes by PCR amplification and scanning by conformation-sensitive gel electrophoresis identifies only *COL1A1* mutations in 15 patients with osteogenesis imperfecta type I: identification of common sequences of null-allele mutations. Am J Hum Genet 62: 98–110.
4. Forlino A, Cabral WA, Barnes AM, Marini JC (2011) New perspectives on osteogenesis imperfecta. Nat Rev Endocrinol 7: 540–557.
5. Thompson EM, Young ID, Hall CM, Pembrey ME (1987) Recurrence risks and prognosis in severe sporadic osteogenesis imperfecta. J Med Genet 24: 390–405.
6. Cohn DH, Starman BJ, Blumberg B, Byers PH (1990) Recurrence of lethal osteogenesis imperfecta due to parental mosaicism for a dominant mutation in a human type I collagen gene (*COL1A1*). Am J Hum Genet 46: 591–601.
7. Cohen-Solal L, Bonaventure J, Maroteaux P (1991) Dominant mutations in familial lethal and severe osteogenesis imperfecta. Hum Genet 87: 297–301.
8. Morello R, Bertin TK, Chen Y, Hicks J, Tonachini L, et al. (2006) CRTAP is required for prolyl 3- hydroxylation and mutations cause recessive osteogenesis imperfecta. Cell 127: 291–304.
9. Barnes AM, Chang W, Morello R, Cabral WA, Weis M, et al. (2006) Deficiency of cartilageassociated protein in recessive lethal osteogenesis imperfecta. N Engl J Med 355: 2757–2764.
10. Cabral WA, Chang W, Barnes AM, Weis M, Scott MA, et al. (2007) Prolyl 3-hydroxylase 1 deficiency causes a recessive metabolic bone disorder resembling lethal/severe osteogenesis imperfecta. Nat Genet 39: 359–365.
11. van Dijk FS, Nesbitt IM, Zwikstra EH, Nikkels PG, Piersma SR, et al. (2009) *PPIB* mutations cause severe osteogenesis imperfecta. Am J Hum Genet 85: 521–527.
12. Barnes AM, Carter EM, Cabral WA, Weis M, Chang W, et al. (2010) Lack of cyclophilin B in osteogenesis imperfecta with normal collagen folding. N Engl J Med 362: 521–528.
13. Christiansen HE, Schwarze U, Pyott SM, AlSwaid A, Al Balwi M, et al. (2010) Homozygosity for a missense mutation in *SERPINH1*, which encodes the collagen chaperone protein HSP47, results in severe recessive osteogenesis imperfecta. Am J Hum Genet 86: 389–398.
14. Alanay Y, Avaygan H, Camacho N, Utine GE, Boduroglu K, et al. (2010) Mutations in the gene encoding the RER protein FKBP65 cause autosomal-recessive osteogenesis imperfecta. Am J Hum Genet 86: 551–559.
15. Lapunzina P, Aglan M, Temtamy S, Caparrós-Martín JA, Valencia M, et al. (2010) Identification of a frameshift mutation in Osterix in a patient with recessive osteogenesis imperfecta. Am J Hum Genet 87: 110–114.
16. Becker J, Semler O, Gilissen C, Li Y, Bolz HJ, et al. (2011) Exome sequencing identifies truncating mutations in human *SERPINF1* in autosomal-recessive osteogenesis imperfecta. Am J Hum Genet 88: 362–371.
17. van Dijk FS, Byers PH, Dalgleish R, Malfait F, Maugeri A, et al. (2011) EMQN best practice guidelines for the laboratory diagnosis of osteogenesis imperfecta. Eur J Hum Genet 20: 11–19.
18. Pyott SM, Schwarze U, Christiansen HE, Pepin MG, Leistritz DF, et al. (2011) Mutations in PPIB (cyclophilin B) delay type I procollagen chain association and result in perinatal lethal to moderate osteogenesis imperfecta phenotypes. Hum Mol Genet 20: 1595–1609.
19. Marini JC, Cabral WA, Barnes AM, Chang W (2007) Components of the collagen prolyl 3- hydroxylation complex are crucial for normal bone development. Cell Cycle 6: 1675–1681.
20. Vranka JA, Sakai LY, Bächinger HP (2004) Prolyl 3-hydroxylase 1, enzyme characterization and identification of a novel family of enzymes. J Biol Chem 279: 23615–23621.
21. Chang W, Barnes AM, Cabral WA, Bodurtha JN, Marini JC (2010) Prolyl 3-hydroxylase 1 and CRTAP are mutually stabilizing in the endoplasmic reticulum collagen prolyl 3-hydroxylation complex. Hum Mol Genet 19: 223–234.
22. Baldridge D, Schwarze U, Morello R, Lennington J, Bertin TK, et al. (2008) *CRTAP* and *LEPRE1* mutations in recessive osteogenesis imperfecta. Hum Mutat 29: 1435–1442.
23. Willaert A, Malfait F, Symoens S, Gevaert K, Kayserili H, et al. (2009) Recessive osteogenesis imperfecta caused by *LEPRE1* mutations: clinical documentation and identification of the splice form responsible for prolyl 3-hydroxylation. J Med Genet 46: 233–241.